# PRICING OF SPREAD AND EXCHANGE OPTIONS IN A ROUGH JUMP-DIFFUSION MARKET

Donatien Hainaut

LIDAM Discussion Paper ISBA
2022 / 12

UCLouvain

LiDAM
ISBA | Louvain Institute of Data Analysis and Modeling in economics and statistics

**ISBA**

Voie du Roman Pays 20 - L1.04.01

B-1348 Louvain-la-Neuve

Email : lidam-library@uclouvain.be

https://uclouvain.be/en/research-institutes/lidam/isba/publication.html

# Pricing of spread and exchange options in a rough jump-diffusion market

Donatien Hainaut*
UCLouvain, LIDAM-ISBA, Belgium

March 24, 2022

**Abstract**

This article studies the pricing of spread and exchange options in a market made up of two risky assets driven by a rough Heston model with jumps. Firstly, we rewrite this non-Markov model as an infinite dimensional Markov process. We next consider a finite dimensional approximation and show that the characteristic function of log-returns admits a representation in terms of forward differential equations. By passing to the limit, we infer that the characteristic function of the rough jump Heston model depends on a hybrid system of ordinary and fractional differential equations. Bivariate options are next priced with a one or two dimensional discrete Fourier Transform. We conclude by a numerical illustration analyzing the impact of roughness on exchange and spread options.

Keywords: Rough volatility, fractional Brownian motion, Heston model, spread options.

## 1 Introduction

Spread and exchange options are popular financial instruments due to their ability to mitigate unfavourable movements in two indexes. The literature on applications of spread options is extensive and we refer to Carmona and Durrleman [7] for a review and applications of spread options to energy trading.

Despite their popularity, the valuation of options written on two underlying assets is a challenging task. Even if Margrabe [19] has proposed a simple formula for exchange options in a geometric Brownian setting, most of spread options may not be priced analytically. Instead we have to rely on approximations or numerical methods. For instance, Kirk [17] presents an analytical approximation that performs well in practice. Li et al. [18] and Bjerksund & Stensland [5] provide lower and upper bounds for the spread option price that produce accurate analytical approximation formulas in log-normal asset models. Deelstra et al. [8]

*Postal address: Voie du Roman Pays 20, 1348 Louvain-la-Neuve (Belgium). E-mail to: donatien.hainaut(at)uclouvain.be

deal with the problem of pricing general Asian basket spread options and propose an approximation formulae based on comonotonicity theory. Pasricha and Goel [22] find a closed form expression for the pricing of vulnerable power exchange options.

Amongst numerical methods, approaches based on the discrete fast Fourier transform (DFT) have met a large success. For instance, Dempster and Hong [9] introduce a numerical integration method for spread options based on two-dimensional Fourier transforms that was shown to be efficient when the asset price processes are GBMs or have stochastic volatility. Hurd and Zhou [16] propose a new formula for general spread option pricing based on Fourier analysis of the payoff function. Alfeus and Schlögl [3] compare the Hurd and Zhou approach to the lower bound approximation formula of Caldana and Fusai [6]. Alternative valuation methods rely on Monte-Carlo methods such as Sun Y. and Xu C. [23] who propose a hybrid Monte Carlo variance reduction method for pricing basket options.

On the other hand, rough asset dynamics recently received a great deal of attention in finance because they are consistent with empirical estimates of stock price volatility. In a rough model, as proposed in the seminal article of Gatheral et al. [14], the variance is driven by a fractional Brownian motion with a Hurst index $H < 1/2$. Bayer et al. [4] study option pricing under rough volatility. El Euch and Rosenbaum [12] and El Euch et al. [12] approximate the fBm by an integral with respect to a standard Bm in a Heston model and study option hedging strategies in this framework. El Euch and Rosenbaum [13] establish the characteristic of a rough Heston process. Abi Jaber et al. [1] show that rough models belong to the family of Affine Volterra processes. Abi Jaber and El Euch [2] characterize the Markovian and affine structure of the Volterra Heston model in terms of an infinite-dimensional forward process. We can also cite Dupret et al. [10] who value the impact of rough volatility on long-term annuities or Dupret and Hainaut [11] who study the performance of constant proportion portfolio insurance in a rough market. When assets exhibit long-range memory, Mehrdoust et al. [20] study the pricing of options in a mixed fractional Heston model for a Hurst index $H \in (\frac{3}{4}, 1)$.

This article contributes to the literature on rough models in several directions. To the best of our knowledge, this is the first that investigates the pricing of spread and exchange options in a rough framework. We also extend the rough Heston model by adding jumps in asset dynamics. From a methodological point of view, we express the joint characteristic function of log-returns in terms of solutions of fractional differential equations. Compared to the existing literature, we prove this result with an approach based on a discretization scheme similar to the one of Abi Jaber and El Euch [2] . The characteristic function of log-return processes present similarities with the one of the rough Heston model obtained by El Euch and Rosenbaum ([13]) by considering the limit of nearly unstable Hawkes processes. Our method for establishing such a result is nevertheless simple and novel since it is based on a discrete approximation of Riemann-Liouville derivatives.

The structure of this article is as follows. We start by presenting the rough log-return processes and remind its relation with the fractional Brownian motion. Since the variance is not a semi-martingale, we cannot rely on Itô calculus to study the properties of the model.

Nevertheless we show that the model admits an infinite dimensional Markov representation that we approximate by discretization in Section 4. In this discrete setting, the characteristic function of log-return processes is computable by solving backward ODE's. We find the characteristic functions under the risk neutral measure and under a pricing measure using one risky asset as numeraire. Nevertheless, these functions do not admit any limit when the number of discretization steps increases. To tackle this issue, we express in Section 5, the approached characteristic functions with forward ODE's. In Section 6, we reformulate them in term of discretized fractional derivatives and find the characteristic function of log-returns by considering the limit. Section 7 details the pricing methods of spread and exchange options whereas Section 8 concludes with a numerical illustration.

# 2 The financial market and bivariate options

We consider a financial market made of two stocks and one risk free asset. The risk free rate asset, noted $S_t^{(0)}$, earns a constant return, $r$ such that $dS_t^{(0)}/S_t^{(0)} = r\,dt$. The stock price processes, denoted by $\left(S_t^{(1)}\right)_{t\geq 0}$ and $\left(S_t^{(2)}\right)_{t\geq 0}$, are defined on a probability space $(\Omega, \mathcal{F}, \mathbb{Q})$ where $\mathbb{Q}$ is the pricing measure. If $\odot$ is the elementwise product, prices of assets $\left(S_t^{(1)}\right)_{t\geq 0}$ and $\left(S_t^{(2)}\right)_{t\geq 0}$ are ruled by the following stochastic differential equations (SDE):

$$\begin{pmatrix} dS_t^{(1)}/S_t^{(1)} \\ dS_t^{(2)}/S_t^{(2)} \end{pmatrix} = \left(r - \boldsymbol{\lambda} \odot (\boldsymbol{\varphi}(1) - 1)\right) dt + \boldsymbol{\Sigma}_{1:2,.} \sqrt{V_t} d\boldsymbol{W}_t + d\boldsymbol{L}_t \,, \tag{1}$$

where $\boldsymbol{\lambda} \in \mathbb{R}^{+2}$, $\boldsymbol{\varphi}(1) \in \mathbb{R}^2$ are vectors and $\boldsymbol{\Sigma}_{1:2,.}$ is a $2{\times}3$ matrix of real numbers:

$$\boldsymbol{\lambda} = \begin{pmatrix} \lambda_1 \\ \lambda_2 \end{pmatrix}, \; \boldsymbol{\varphi}(1) = \begin{pmatrix} \varphi^{(1)}(1) \\ \varphi^{(2)}(1) \end{pmatrix}, \; \boldsymbol{\Sigma}_{1:2,.} = \begin{pmatrix} \sigma_{11} & \sigma_{12} & \sigma_{13} \\ \sigma_{21} & \sigma_{22} & \sigma_{23} \end{pmatrix}.$$

The process $\boldsymbol{W}_t = \left(W_t^{(1)}, W_t^{(2)}, W_t^{(3)}\right)^\top$ is a vector of independent Brownian motions whereas $\boldsymbol{L}_t = \left(L_t^{(1)}, L_t^{(2)}\right)^\top$ is a bivariate compound Poisson process,

$$L_t^{(i)} = \sum_{k=1}^{N_t^{(i)}} \left(e^{J_k^{(i)}} - 1\right), \; i = 1, 2 \,. \tag{2}$$

In this last equation, $\left(N_t^{(i)}\right)_{t\geq 0}$ for $i = 1, 2$, are Poisson processes with intensities $\boldsymbol{\lambda}$. The jump sizes $\boldsymbol{J} = (J^{(1)}, J^{(2)})$ are double exponential random variables on $\mathbb{R}$. The probability density functions (pdf's) of jumps are respectively

$$\begin{aligned} f_{J^{(1)}}(x) &= p_{11}\eta_{11}e^{-\eta_{11}x}1_{\{x\geq 0\}} + p_{12}\eta_{12}e^{\eta_{12}x}1_{\{x<0\}} \,, \\ f_{J^{(2)}}(x) &= p_{21}\eta_{21}e^{-\eta_{21}x}1_{\{x\geq 0\}} + p_{22}\eta_{22}e^{\eta_{22}x}1_{\{x<0\}} \,, \end{aligned}$$

where $\eta_{i,j} \geq 0$ for $i,j = 1,2$ and $p_{11}, p_{12}$ (resp. $p_{12}, p_{22}$) are the probabilities of observing a positive and negative jumps of $J^{(1)}$ (resp. $J^{(2)}$). The moment generating functions of jumps are noted $\varphi^{(i)}(\omega)$,

$$\varphi^{(i)}(\omega) = \mathbb{E}\left(e^{\omega J^{(i)}}\right) \quad = \quad p_{i1}\frac{\eta_{i1}}{\eta_{i1}-\omega} + p_{i2}\frac{\eta_{i2}}{\eta_{i2}+\omega} \; i = 1,2,$$

for $\omega \in [-\eta_{i2}, \eta_{i1}]$ or $\omega \in \mathbb{C}^-$. Jump processes in Equation (1) are compensated. Therefore, the expected instantaneous returns under the pricing measure $\mathbb{Q}$ are equal to the risk free rate $\mathbb{E}\left(dS_t^{(i)}/S_t^{(i)} \,|\, \mathcal{F}_{t-}\right) = rdt$. The univariate process $(V_t)_{t\geq 0}$ represents the systemic variance and we assume that its dynamic is comparable to the one of a rough fractional Brownian motion (fBm). Let $H$, $0 \leq H \leq 1$, be referred to as the Hurst parameter. The stochastic process $\left(B_t^H\right)_{t\geq 0}$ is a fractional Brownian motion (fBm) of order $H$ if $B_t^H$ is an $\mathcal{F}_t$-measurable Gaussian process such that $\mathbb{E}\left(B_t^H\right) = 0$ and for $t, s \in \mathbb{R}^+$, the autocovariance is:

$$\mathbb{E}\left(B_t^H B_s^H\right) \quad = R_H(t,s) = \quad \frac{1}{2}\left(t^{2H} + s^{2H} - |t-s|^{2H}\right) \tag{3}$$

It follows from (3) and from Kolmogorov's continuity criterion that the sample paths of $B_t^H$ are continuous with probability one but nowhere differentiable. From the definition,we infer that the variance of the fBm is equal to

$$\mathbb{V}\left(B_t^H\right) \quad = \quad t^{2H}\,.$$

The fractional process is also self-similar i.e. the process $a^{-H}B_{at}^H$ has the same law as $B_t^H$ for $a > 0$. The fBm can be rewritten as an integral with respect to a Bm, $(W_t)_{t\geq 0}$, which highlights the memory of the process:

$$B_t^H = \frac{1}{C_H}\left[\int_{-\infty}^0 \left((t-s)^{H-\frac{1}{2}} - (-s)^{H-\frac{1}{2}}\right) dW_s + \int_0^t (t-s)^{H-\frac{1}{2}}\, dW_s\right] \tag{4}$$

where $C_H$ is function of the Hurst index. When $H < \frac{1}{2}$, it is natural to only consider the integral on the positive time axis when the Bm is not defined before time zero i.e. :

$$B_t^H \quad \approx \quad \frac{1}{\Gamma(\alpha)}\int_0^t (t-s)^{\alpha-1}\, dW_s \tag{5}$$

where $\alpha = H + 1/2 \in (\frac{1}{2}, 1)$. This approach was used by El Euch and Rosenbaum ([12]) who study a rough version of the Heston model. In this article, the volatility based on the approximation (5) of the fractional Brownian motion is ruled by

$$\begin{aligned} V_t = V_0 + \frac{1}{\Gamma(\alpha)}\int_0^t (t-s)^{\alpha-1}\kappa\left(\theta - V_s\right) ds \\ + \frac{1}{\Gamma(\alpha)}\int_0^t (t-s)^{\alpha-1}\sqrt{V_s}\boldsymbol{\Sigma}_{3,.} d\boldsymbol{W}_s\,. \end{aligned} \tag{6}$$

where $\alpha \in (\frac{1}{2}, 1)$, $\theta, \kappa \in \mathbb{R}^+$ and $\boldsymbol{\Sigma}_{3,.} = (\sigma_{3,1}, \sigma_{32}, \sigma_{33}) \in \mathbb{R}^3$ (notice that $\boldsymbol{\Sigma}_{3,.}$ is a row vector). This process is rough in the sense that its differential is not defined ($dV_t = \infty$). When $\alpha = 1$, the $V_t$ is a Markov process with a Cox-Ingersoll-Ross (CIR) dynamic:

$$dV_t = \kappa \left(\theta - V_t\right) dt + \sqrt{V_t} \boldsymbol{\Sigma}_{3,.} d\boldsymbol{W}_t \,. \tag{7}$$

We denote by $(\mathcal{G}_t)_{t\geq 0}$ the filtration of $V_t$. The filtration $\mathcal{F}_t$ is the augmented filtration and gather information about all previous processes.

This article studies the pricing of two popular bivariate contingent claims: the spread and the exchange options. We denote by $T$ and $K$, the option expiry date and the strike price whereas $\pi_1, \pi_2 \in \mathbb{R}^+$ are weights. The European spread option derives its value from the difference, or spread, between the prices of two assets. A call (resp. put) spread option delivers the payoff $\left(\pi_1 S_T^{(1)} - \pi_2 S_T^{(2)} - K\right)_+$ (resp. $\left(K - \pi_1 S_T^{(1)} - \pi_2 S_T^{(2)}\right)_+$) at expiry. The valuation of such an option requires to determine the probability density functions (pdf) of log-returns. Let us denote by $f_{\boldsymbol{X}_T}(\boldsymbol{x})$, this bivariate pdf of log-returns where $\boldsymbol{X}_t = (X_t^{(1)}, X_t^{(2)})$ with $X_t^{(1)} = \ln \frac{S_t^{(1)}}{S_0^{(1)}}$ and $X_t^{(2)} = \ln \frac{S_t^{(2)}}{S_0^{(2)}}$ under $\mathbb{Q}$. The value of the call-spread option is then equal to the expected discounted payoff

$$\begin{aligned} P^{spread} &= e^{-rT} \mathbb{E}\left( \left(\pi_1 S_T^{(1)} - \pi_2 S_T^{(2)} - K\right)_+ | \, \mathcal{F}_0 \right) \\ &= e^{-rT} \int_{D^{spread}} \left(\pi_1 S_0^{(1)} e^{x_1} - \pi_2 S_0^{(2)} e^{x_2} - K\right) f_{\boldsymbol{X}_T}(\boldsymbol{x}) \, dx_1 dx_2 \end{aligned} \tag{8}$$

where $D^{spread} = \{\boldsymbol{x} = (x_1, x_2) \in \mathbb{R}^2 \,|\, \pi_1 S_0^{(1)} e^{x_1} - \pi_2 S_0^{(2)} e^{x_2} \geq K\}$ is the domain on which the payoff is positive. The following sections focus on the computation of $f_{\boldsymbol{X}_T}(\boldsymbol{x})$.

Exchange options allow to exchange a risky asset for another risky asset at maturity. The payoff of such options is either $(\pi_1 S_T^{(1)} - \pi_2 S_T^{(2)})_+$ or $\left(\pi_2 S_T^{(2)} - \pi_1 S_T^{(1)}\right)_+$. This type of option being nothing else than a spread option with a null strike, its price can be calculated by integrating the bivariate density of log-returns as in Equation (8). An alternative approach consists to find the pdf of the log-returns difference under a measure using one of the two risky assets as numeraire. For instance, let us consider the following exchange option

$$P^{exchange} \;=\; e^{-rT} \mathbb{E}\left( \left(\pi_1 S_T^{(1)} - \pi_2 S_T^{(2)}\right)_+ | \, \mathcal{F}_0 \right) \,. \tag{9}$$

For such an option, we denote by $\mathbb{S}$ the measure with $S_t^{(1)}$ as numeraire and $\left.\frac{d\mathbb{S}}{d\mathbb{Q}}\right|_T = \frac{S_T^{(1)} e^{-rT}}{S_0^{(1)}}$. Using the corresponding change of measure leads to the following equivalent formulation:

$$\begin{aligned} P^{exchange} &= \pi_1 S_0^{(1)} \mathbb{E}^{\mathbb{S}}\left( \left(1 - \frac{\pi_2 S_T^{(2)}}{\pi_1 S_T^{(1)}}\right)_+ | \, \mathcal{F}_0 \right) \\ &= \int_{D^{exchange}} \left(\pi_1 S_0^{(1)} - \pi_2 S_0^{(2)} e^{x}\right) f^{\mathbb{S}}_{X_T^{(2)} - X_T^{(1)}}(x) \, dx \end{aligned}$$

where $f^{\mathbb{S}}_{X_T^{(2)}-X_T^{(1)}}(x)$ is the pdf of $\ln\frac{S_T^{(2)}}{S_0^{(2)}}-\ln\frac{S_T^{(1)}}{S_0^{(1)}}$ under the $\mathbb{S}$ measure and $D^{exchange}=\{x\in\mathbb{R}\,|\,\pi_2 S_0^{(2)}e^x\leq\pi_1 S_0^{(1)}\}$ is the domain on which the payoff is positive.

The following sections focus on the calculation of densities $f_{\boldsymbol{X}_T}(\boldsymbol{x})$ and $f^{\mathbb{S}}_{X_T^{(2)}-X_T^{(1)}}(x)$ needed to value spread and exchange options. This is done in several steps. Firstly, we reformulate the rough dynamics of $V_t$ as an infinite dimensional Markov process that is next approximated by a finite model. In the second step, we use the Itô's lemma and approach the characteristic functions of log-returns and of their difference. By taking the limit, we find that non-approximated characteristic functions are computable by solving ordinary and fractional differential equations. Finally, options are priced by inverting numerically characteristic functions with a standard discrete fast Fourier transform (DFT).

# 3 An equivalent infinite dimensional Markov process

The variance process $V_t$, is not Markov as its current value depends on the sample path up to time $t$. Nevertheless, we can rewrite it as an infinite dimensional Markov process. For this purpose, the integrand in Eq. (6) is developped as an integral,

$$\begin{aligned}(t-u)^{\alpha-1} &= \frac{1}{\Gamma(1-\alpha)}\int_0^\infty \frac{e^{-(t-u)\xi}}{\xi^\alpha}d\xi \\ &:= \int_0^\infty e^{-(t-u)\xi}\gamma(d\xi)\,,\end{aligned}$$

where $\gamma(d\xi):=\frac{\xi^{-\alpha}}{\Gamma(1-\alpha)}\,d\xi$ is a measure on $\mathbb{R}^+$. This allows to reformulate the process $V_t$ as an integral of an infinity of Ornstein-Uhlenbeck processes. Using the Fubini theorem to develop the intensity as an integral with respect to $\gamma(.)$ leads indeed to the following expression:

$$\begin{aligned}V_t &= V_0+\frac{1}{\Gamma(\alpha)}\int_0^\infty\int_0^t e^{-(t-s)\xi}\kappa\left(\theta-V_s\right)ds\,\gamma(d\xi) \\ &\quad+\frac{1}{\Gamma(\alpha)}\int_0^\infty\int_0^t e^{-(t-s)\xi}\sqrt{V_s}\boldsymbol{\Sigma}_{3,.}d\boldsymbol{W}_s\,\gamma(d\xi).\end{aligned} \tag{10}$$

Let us now define a family of processes $Y_t^{(\xi)}$ indexed by $\xi\geq 0$ such that

$$Y_t^{(\xi)}=\int_0^t e^{-(t-s)\xi}\kappa\left(\theta-V_s\right)ds+\int_0^t e^{-(t-s)\xi}\sqrt{V_s}\boldsymbol{\Sigma}_{3,.}d\boldsymbol{W}_s\,.$$

These processes are strictly positive, Markov and revert to $\frac{\kappa}{\xi}\left(\theta-V_t\right)$ with a speed $\xi$. Their differential is provided by the next SDE:

$$dY_t^{(\xi)} = \xi\left(\frac{\kappa}{\xi}\left(\theta-V_t\right)-Y_t^{(\xi)}\right)dt+\sqrt{V_t}\,\boldsymbol{\Sigma}_{3,.}d\boldsymbol{W}_t\,.$$

From Equation (10), the intensity $V_t$ is then equal an integral of $Y_t^{(\xi)}$ with respect to the measure $\gamma(.)$:

$$V_t=V_0+\frac{1}{\Gamma(\alpha)}\int_0^\infty Y_t^{(\xi)}\,\gamma(d\xi)\,. \tag{11}$$

This expression does not depend anymore upon information prior to $t$. This relation emphasizes that $\lambda_t$ and $\left(Y_t^{(\xi)}\right)_{\xi\in\mathbb{R}^+}$ form well an infinite dimensional Markov process. As we need the Itô's calculus for further developments, we have to approach the infinite dimensional model by a finite one.

# 4 Finite dimensional approximation

Instead of considering an infinity of processes $\left(Y_t^{(\xi)}\right)_{t\geq 0}$, we approach the model by a finite number of equivalent ones. The main advantage of this approach is that we can next rely on the Itô's calculus to approximate the characteristic function of stock log-returns. The key step consists to approach $\gamma(.)$ by a discrete measure with a finite numbers of atoms. For this purpose we consider a partition $\mathcal{E}^{(n)} := \{0 < \xi_0^{(n)} < \xi_1^{(n)} < ... < \xi_n^{(n)} < \infty\}$. The mid point of each interval $(\xi_i^{(n)}, \xi_{i+1}^{(n)})$ is

$$b_{k+1} \quad = \quad \frac{\xi_k^{(n)} + \xi_{k+1}^{(n)}}{2} \tag{12}$$

and the mass of corresponding atoms is the measure of intervals of the partition:

$$m_{k+1} = \int_{\xi_k^{(n)}}^{\xi_{k+1}^{(n)}} d\gamma(z) = \frac{\left(\left(\xi_{k+1}^{(n)}\right)^{1-\alpha} - \left(\xi_k^{(n)}\right)^{1-\alpha}\right)}{\Gamma(1-\alpha)(1-\alpha)}\,, \tag{13}$$

for $k = 0, ..., n-1$. The discrete measure for a partition of size $n$ is defined by

$$\bar{\gamma}(z) = \sum_{k=1}^{n} m_k \delta_{b_k}(z)\,, \tag{14}$$

where $\delta_{b_k}(z)$ is the Dirac measure located at point $b_k$. We consider that the following assumption holds for the partition $\mathcal{E}^{(n)}$ :

- $\xi_0^{(n)} \to 0$ and $\xi_n^{(n)} \to \infty$ when $n \to \infty$.
- $\max|\xi_{i+1}^{(n)} - \xi_i^{(n)}| \to 0$ when $n \to \infty$.
- $\mathcal{E}^{(n)} \subset \mathcal{E}^{(n+1)}$.

These assumptions guarantee that for any function $f(.)$ integrable with respect to $\gamma(.)$, $\lim_{n\to\infty} \int_0^\infty f(z)\, d\bar{\gamma}(z) = \int_0^\infty f(z)\, d\gamma(z)$. To lighten further developments, we adopt the following notations $Y_t^{(k)} := Y_t^{(b_k)}$ for $k = 1, ..., n$. The $Y_t^{(k)}$'s under $\mathbb{Q}$ are such that

$$Y_t^{(k)} = \int_0^t e^{-(t-s)b_k} \kappa\left(\theta - \bar{V}_s\right) ds + \int_0^t e^{-(t-s)b_k} \sqrt{\bar{V}_s}\, \mathbf{\Sigma}_{3,.} d\boldsymbol{W}_s\,.$$

and $\bar{V}_t = V_0 + \frac{1}{\Gamma(\alpha)} \sum_{k=1}^{n} Y_t^{(k)} m_k$ is the process approximating $V_t$. The differential of processes $Y_t^{(k)}$ is given by

$$dY_t^{(k)} = \left(\kappa\left(\theta - \bar{V}_t\right) - b_k Y_t^{(k)}\right) dt + \sqrt{\bar{V}_t}\, \boldsymbol{\Sigma}_{3,.} d\boldsymbol{W}_t\,, \tag{15}$$

for $k = 1, ..., n$. On the other hand, the dynamics of the rough approached volatility, denoted by $\bar{V}_t$, is

$$d\bar{V}_t = \frac{1}{\Gamma(\alpha)} \sum_{k=1}^{n} m_k \left(\kappa\left(\theta - \bar{V}_t\right) - b_k Y_t^{(k)}\right) dt + \frac{\sqrt{\bar{V}_t}}{\Gamma(\alpha)} \sum_{k=1}^{n} m_k\, \boldsymbol{\Sigma}_{3,.} d\boldsymbol{W}_t\,. \tag{16}$$

Stock prices are respectively denoted by $\left(\bar{S}_t^{(1)}\right)_{t\geq 0}$ and $\left(\bar{S}_t^{(2)}\right)_{t\geq 0}$ in the finite dimensional model. To lighten further developments, we need to introduce a new bivariate jump process, $\boldsymbol{L}_t^X = \left(L_t^{X(1)}, L_t^{X(2)}\right)$ where

$$L_t^{X(i)} = \sum_{k=1}^{N_t^{(i)}} J_k^{(i)} \quad i = 1, 2. \tag{17}$$

This bivariate process represents the jumps of asset log-returns. We use the Itô's lemma to infer $\bar{\boldsymbol{S}}_t = \left(\bar{S}_t^{(1)}, \bar{S}_t^{(2)}\right)^\top$ solving Equation (1):

$$\begin{aligned}\bar{\boldsymbol{S}}_t &= \bar{\boldsymbol{S}}_0 \odot \exp\Bigg(\left(\boldsymbol{r} - \boldsymbol{\lambda} \odot (\boldsymbol{\varphi}(1) - 1)\right) t - \frac{1}{2} diag(\boldsymbol{\Sigma}_{1:2,.} \boldsymbol{\Sigma}_{1:2,.}^\top) \int_0^t \bar{V}_s ds \\ &\quad + \boldsymbol{\Sigma}_{1:2,.} \int_0^t \sqrt{\bar{V}_s} d\boldsymbol{W}_s + \boldsymbol{L}_t^X \Bigg)\,,\end{aligned}$$

where $\odot$ is the pointwise product. The SDE ruling the (approached) log-returns under $\mathbb{Q}$, noted $\bar{\boldsymbol{X}}_t = \left(\bar{X}_t^{(1)}, \bar{X}_t^{(2)}\right)$ where $\bar{X}_t^{(1)} = \ln(\bar{S}_t^{(1)}/\bar{S}_0^{(1)})$ and $\bar{X}_t^{(2)} = \ln(\bar{S}_t^{(2)}/\bar{S}_0^{(2)})$ are therefore solution of

$$\begin{aligned}d\bar{\boldsymbol{X}}_t &= \left(\boldsymbol{r} - \boldsymbol{\lambda} \odot (\boldsymbol{\varphi}(1) - 1) - \frac{1}{2} diag\left(\boldsymbol{\Sigma}_{1:2,.} \boldsymbol{\Sigma}_{1:2,.}^\top\right) \bar{V}_t\right) dt \\ &\quad + \boldsymbol{\Sigma}_{1:2,.} \sqrt{\bar{V}_t} d\boldsymbol{W}_t + d\boldsymbol{L}_t^X\,.\end{aligned} \tag{18}$$

As seen in Section 2, we can appraise exchange options under an alternative measure using one risky asset as numeraire. For this reason, we need the dynamics of $\bar{\boldsymbol{X}}_t$ under the $\mathbb{S}$ measure with $\bar{S}_t^{(1)}$ as numeraire. If $\boldsymbol{e}_1 = (1, 0)^\top$ and $\boldsymbol{e}_2 = (0, 1)^\top$, the change of measure from $\mathbb{Q}$ to $\mathbb{S}$ is defined by the ratio $\frac{d\mathbb{S}}{d\mathbb{Q}}\Big|_t = \frac{\bar{S}_t^{(1)} \bar{S}_0^{(0)}}{\bar{S}_0^{(1)} \bar{S}_t^{(0)}}$ that is developped as

$$\begin{aligned}\frac{d\mathbb{S}}{d\mathbb{Q}}\Big|_t &= \exp\Bigg(-\frac{1}{2} \int_0^t \boldsymbol{e}_1^\top \boldsymbol{\Sigma}_{1:2,.} \boldsymbol{\Sigma}_{1:2,.}^\top \boldsymbol{e}_1 \bar{V}_s ds - \int_0^t \left(-\boldsymbol{e}_1^\top \boldsymbol{\Sigma}_{1:2,.} \sqrt{\bar{V}_s}\right) d\boldsymbol{W}_s \\ &\quad - \lambda_1 \left(\varphi^{(1)}(1) - 1\right) t + \sum_{k=1}^{N_t^{(1)}} J_k^{(1)} \Bigg)\,.\end{aligned}$$

We recognize a Radon-Nykodym derivative such that $d\boldsymbol{W}_t^{\mathbb{S}} = d\boldsymbol{W}_t - \boldsymbol{\Sigma}_{1:2,.}^{\top}\boldsymbol{e}_1\sqrt{\bar{V}_t}dt$ is a Brownian motion under $\mathbb{S}$. Under $\mathbb{S}$, we check in appendix A, that $L_t^{X(1)}$ is still a jump process but $N_t^{(1)}$ is a Poisson process with a modified parameter $\lambda_1^{\mathbb{S}} = \lambda_1\varphi^{(1)}(1)$. Jumps of $X_t^{(1)}$ under $\mathbb{S}$, noted $J^{\mathbb{S}\,(1)}$, are double exponential random variable with modified parameters

$$p_{11}^{\mathbb{S}} = p_{11}\frac{\eta_{11}}{\varphi^{(1)}(1)\left(\eta_{11}-1\right)} \quad , \quad p_{12}^{\mathbb{S}} = p_{12}\frac{\eta_{12}}{\varphi^{(1)}(1)\left(\eta_{12}+1\right)}, \tag{19}$$

$$\eta_{11}^{\mathbb{S}} = \eta_{11} - 1 \quad , \quad \eta_{12}^{\mathbb{S}} = \eta_{12} + 1\,. \tag{20}$$

The distribution of jumps of $X_t^{(2)}$ under $\mathbb{S}$ does not differ from the one under the risk neutral measure. In later developments, we need the following notations

$$\boldsymbol{\lambda}^{\mathbb{S}} = \begin{pmatrix} \lambda_1^{\mathbb{S}} \\ \lambda_2 \end{pmatrix} \quad , \quad \boldsymbol{\varphi}^{\mathbb{S}}(\omega) = \begin{pmatrix} \varphi^{(1)\,\mathbb{S}}(\omega_1) \\ \varphi^{(2)}(\omega_1) \end{pmatrix} , \, \boldsymbol{J}^{\mathbb{S}} = \begin{pmatrix} J_1^{\mathbb{S}} \\ J_2 \end{pmatrix} .$$

It is then easy to chech that log-returns in the finite dimensional model, under the measure $\mathbb{S}$, are solutions of SDE's:

$$\begin{aligned} d\bar{\boldsymbol{X}}_t &= \left(\boldsymbol{r} - \boldsymbol{\lambda}\odot\left(\boldsymbol{\varphi}(1)-1\right)\right)dt + \boldsymbol{\Sigma}_{1:2,.}\sqrt{\bar{V}_t}d\boldsymbol{W}_t^{\mathbb{S}} + d\boldsymbol{L}_t^X \\ &\quad + \bar{V}_t\left(\boldsymbol{\Sigma}_{1:2,.}\boldsymbol{\Sigma}_{1:2,.}^{\top}\boldsymbol{e}_1 - \frac{1}{2}diag\left(\boldsymbol{\Sigma}_{1:2,.}\boldsymbol{\Sigma}_{1:2,.}^{\top}\right)\right)dt\,. \end{aligned} \tag{21}$$

If we denote $\kappa^{\mathbb{S}} = \kappa - \boldsymbol{\Sigma}_{3,.}\boldsymbol{\Sigma}_{1:2,.}^{\top}\boldsymbol{e}_1$, the dynamic under $\mathbb{S}$ of the market variance becomes

$$d\bar{V}_t = \frac{1}{\Gamma(\alpha)}\sum_{k=1}^{n} m_k\left(\kappa\theta - \kappa^{\mathbb{S}}\bar{V}_t - b_k Y_t^{(k)}\right)dt + \frac{\sqrt{\bar{V}_t}}{\Gamma(\alpha)}\sum_{k=1}^{n} m_k\,\boldsymbol{\Sigma}_{3,.}d\boldsymbol{W}_t^{\mathbb{S}}\,, \tag{22}$$

whereas the dynamic of processes $Y_t^{(k)}$ is modified in a similar manner:

$$dY_t^{(k)} = \left(\kappa\theta - \kappa^{\mathbb{S}}\bar{V}_t - b_k Y_t^{(k)}\right)dt + \sqrt{\bar{V}_t}\,\boldsymbol{\Sigma}_{3,.}d\boldsymbol{W}_t^{\mathbb{S}}\,. \tag{23}$$

# 5 Characteristic function of log-returns in the finite dimensional model

In the finite dimensional model, we can take profit of the affine structure of driving processes to infer the characteristic function of stock log-returns. The next proposition shows that this function is computable by solving a system of backward differential equations. We will next find an equivalent representation with forward differential equations that serves in the next section to retrieve the characteristic function of the initial model.

**Proposition 5.1.** *For $\boldsymbol{\omega} = (\omega_1, \omega_2)^{\top} \in \mathbb{C}^{2,-}$ and $0 \leq t \leq s$, the characteristic function of log-returns $\bar{\boldsymbol{X}}_s = (\bar{X}_s^{(1)}, \bar{X}_s^{(2)})$ under the risk neutral measure is*

$$\mathbb{E}\left(e^{\boldsymbol{\omega}^{\top}\bar{\boldsymbol{X}}_s}|\mathcal{F}_t\right) = \exp\left(a(t,s) + c(t,s)\bar{V}_t - \sum_{k=1}^{n} d_k(t,s)Y_t^{(k)} + \boldsymbol{\omega}^{\top}\bar{\boldsymbol{X}}_t\right) \tag{24}$$

*where functions $d_k(t,s)$ are such that*

$$d_k(t,s) = m_k b_k \int_t^s e^{-b_k(u-t)} \frac{c(u,s)}{\Gamma(\alpha)} du \quad k = 1, ..., n\,. \tag{25}$$

*If we define*

$$h_k(t,s) \;\; = \;\; c(t,s) - b_k \int_t^s e^{-b_k(u-t)} c(u,s) du\,,$$

*functions $a(t,s)$, $c(t,s)$ solve the following ordinary differential equations (ODE's):*

$$\partial_t a(t,s) = -\boldsymbol{\omega}^\top (\boldsymbol{r} - \boldsymbol{\lambda} \odot (\boldsymbol{\varphi}(1) - 1)) - \boldsymbol{\lambda}^\top (\boldsymbol{\varphi}(\boldsymbol{\omega}) - 1) - \kappa\theta \sum_{k=1}^n \frac{m_k h_k(t,s)}{\Gamma(\alpha)}\,, \tag{26}$$

*and*

$$\begin{aligned} \partial_t c(t,s) &= \frac{1}{2}\boldsymbol{\omega}^\top diag(\boldsymbol{\Sigma}_{1:2,.}\boldsymbol{\Sigma}_{1:2,.}^\top) - \frac{1}{2}\boldsymbol{\omega}^\top \left(\boldsymbol{\Sigma}_{1:2,.}\boldsymbol{\Sigma}_{1:2,.}^\top\right)\boldsymbol{\omega} \\ &+ \left(\kappa - \boldsymbol{\omega}^\top \boldsymbol{\Sigma}_{1:2,.}\boldsymbol{\Sigma}_{3,.}^\top\right) \sum_{k=1}^n \frac{m_k h_k(t,s)}{\Gamma(\alpha)} - \frac{\boldsymbol{\Sigma}_{3,.}\boldsymbol{\Sigma}_{3,.}^\top}{2} \left(\sum_{k=1}^n \frac{m_k h_k(t,s)}{\Gamma(\alpha)}\right)^2 \end{aligned} \tag{27}$$

*with the terminal conditions $a(s,s) = 0$ and $c(s,s) = 0$.*

**Proof** Let us denote the characteristic function $\mathbb{E}\left(e^{\boldsymbol{\omega}^\top \bar{\boldsymbol{X}}_s} | \mathcal{F}_t\right)$ by $f(t, \bar{\boldsymbol{X}}_t, \bar{V}_t, (Y_t^{(k)})_{k=1,\dots,n})$, the gradient and Hessian of $f$ with respect to $\bar{\boldsymbol{X}}_t$ by $\nabla_{\bar{\boldsymbol{X}}} f$ and $H_{\bar{\boldsymbol{X}}}(f)$,

$$\nabla_{\bar{\boldsymbol{X}}} f = \begin{pmatrix} \partial_{\bar{X}^{(1)}} f \\ \partial_{\bar{X}^{(2)}} f \end{pmatrix} \quad , \quad H_{\bar{\boldsymbol{X}}}(f) = \begin{pmatrix} \partial^2_{\bar{X}^{(1)},\bar{X}^{(1)}} f & \partial^2_{\bar{X}^{(1)},\bar{X}^{(2)}} f \\ \partial^2_{\bar{X}^{(2)},\bar{X}^{(1)}} f & \partial^2_{\bar{X}^{(2)},\bar{X}^{(2)}} f \end{pmatrix}.$$

As the number of stochastic processes is finite, we can rely on Itô's lemma to infer that $f$ is solution of a stochastic differential equation (SDE):

$$\begin{aligned} 0 &= \partial_t f + \nabla_{\bar{\boldsymbol{X}}} f^\top \left(\boldsymbol{r} - \boldsymbol{\lambda} \odot (\boldsymbol{\varphi}(1) - 1) - \frac{1}{2} diag(\boldsymbol{\Sigma}_{1:2,.}\boldsymbol{\Sigma}_{1:2,.}^\top)\bar{V}_t\right) \\ &+ \frac{1}{2} Trace\left(\boldsymbol{\Sigma}_{1:2,.}\boldsymbol{\Sigma}_{1:2,.}^\top H_{\bar{\boldsymbol{X}}}(f)\right)\bar{V}_t + \boldsymbol{\lambda}^\top \mathbb{E}\left(f\left(\bar{\boldsymbol{X}}_t + \boldsymbol{J}\right) - f\right) \\ &+ \partial_{\bar{V}} f \frac{1}{\Gamma(\alpha)} \sum_{k=1}^n m_k \left(\kappa\left(\theta - \bar{V}_t\right) - b_k Y_t^{(k)}\right) + \frac{1}{2}\bar{V}_t \frac{\boldsymbol{\Sigma}_{3,.}\boldsymbol{\Sigma}_{3,.}^\top \left(\sum_{l=1}^n m_l\right)^2}{\Gamma(\alpha)^2} \partial^2_{\bar{V}\bar{V}} f \\ &+ \bar{V}_t \frac{\boldsymbol{\Sigma}_{3,.}\boldsymbol{\Sigma}_{3,.}^\top \sum_{l=1}^n m_l}{\Gamma(\alpha)} \sum_{k=1}^n \partial^2_{\bar{V}Y^{(k)}} f + \frac{\bar{V}_t}{\Gamma(\alpha)} \left(\sum_{k=1}^n m_k \boldsymbol{e}_1^\top \boldsymbol{\Sigma}_{1:2,.}\boldsymbol{\Sigma}_{3,.}^\top\right) \partial^2_{\bar{V}\bar{X}^{(1)}} f \\ &+ \frac{\bar{V}_t}{\Gamma(\alpha)} \left(\sum_{k=1}^n m_k \boldsymbol{e}_2^\top \boldsymbol{\Sigma}_{1:2,.}\boldsymbol{\Sigma}_{3,.}^\top\right) \partial^2_{\bar{V}\bar{X}^{(2)}} f + \sum_{k=1}^n \partial_{Y^{(k)}} f \left(\kappa\left(\theta - \bar{V}_t\right) - b_k Y_t^{(k)}\right) \\ &+ \frac{1}{2}\bar{V}_t \boldsymbol{\Sigma}_{3,.}\boldsymbol{\Sigma}_{3,.}^\top \sum_{k_1=1,k_2=1}^n \partial^2_{Y^{(k_1)}Y^{(k_2)}} f + \bar{V}_t \boldsymbol{e}_1^\top \boldsymbol{\Sigma}_{1:2,.}\boldsymbol{\Sigma}_{3,.}^\top \sum_{k=1}^n \partial^2_{Y^{(k)}\bar{X}^{(1)}} f \\ &+ \bar{V}_t \boldsymbol{e}_2^\top \boldsymbol{\Sigma}_{1:2,.}\boldsymbol{\Sigma}_{3,.}^\top \sum_{k=1}^n \partial^2_{Y^{(k)}\bar{X}^{(2)}} f\,. \end{aligned} \tag{28}$$

By construction, the model has an affine structure, we do the ansatz that $f(.)$ is an exponential function of the form:

$$f(.) \;=\; \exp\left(a(t,s)+c(t,s)\bar{V}_t-\sum_{k=1}^{n}d_k(t,s)Y_t^{(k)}+\omega_1\bar{X}_t^{(1)}+\omega_2\bar{X}_t^{(2)}\right)\,, \tag{29}$$

where $a(t,s)$, $c(t,s)$ and $d_k(t,s)$ are $\mathcal{C}^1$ functions with respect to $t$, for $k=1,...,n$. Injecting the partial derivatives of Equation (29) in Equation (28) leads to the expression

$$\begin{aligned}
&0=\partial_t a+\partial_t c\bar{V}_t-\sum_{k=1}^{n}\partial_t d_k Y_t^{(k)}+\boldsymbol{\omega}^\top\left(\boldsymbol{r}-\boldsymbol{\lambda}\odot\left(\boldsymbol{\varphi}(1)-1\right)\right)\\
&-\frac{1}{2}\left(\boldsymbol{\omega}^\top diag(\boldsymbol{\Sigma}_{1:2,.}\boldsymbol{\Sigma}_{1:2,.}^\top)-\frac{1}{2}\boldsymbol{\omega}^\top\left(\boldsymbol{\Sigma}_{1:2,.}\boldsymbol{\Sigma}_{1:2,.}^\top\right)\boldsymbol{\omega}\right)\bar{V}_t\\
&+\frac{\bar{V}_t}{\Gamma(\alpha)}\left(\sum_{k=1}^{n}m_k\,\boldsymbol{\omega}^\top\boldsymbol{\Sigma}_{1:2,.}\boldsymbol{\Sigma}_{3,.}^\top\right)c+\frac{c}{\Gamma(\alpha)}\sum_{k=1}^{n}m_k\left(\kappa\left(\theta-\bar{V}_t\right)-b_kY_t^{(k)}\right)\\
&+\frac{1}{2}\bar{V}_t\frac{\left(\sum_{l=1}^{n}m_l\right)^2\boldsymbol{\Sigma}_{3,.}\boldsymbol{\Sigma}_{3,.}^\top}{\Gamma(\alpha)^2}c^2-\bar{V}_t\frac{\boldsymbol{\Sigma}_{3,.}\boldsymbol{\Sigma}_{3,.}^\top\sum_{l=1}^{n}m_l}{\Gamma(\alpha)}\sum_{k=1}^{n}cd_k\\
&-\sum_{k=1}^{n}d_k\,\left(\kappa\left(\theta-\bar{V}_t\right)-b_kY_t^{(k)}\right)+\frac{1}{2}\bar{V}_t\boldsymbol{\Sigma}_{3,.}\boldsymbol{\Sigma}_{3,.}^\top\sum_{k_1=1,k_2=1}^{n}d_{k_1}d_{k_2}\\
&-\bar{V}_t\left(\boldsymbol{\omega}^\top\boldsymbol{\Sigma}_{1:2,.}\boldsymbol{\Sigma}_{3,.}^\top\right)\sum_{k=1}^{n}d_k+\boldsymbol{\lambda}^\top\left(\boldsymbol{\varphi}(\boldsymbol{\omega})-1\right)\,.
\end{aligned}$$

This equation is satisfied if and only if coefficients multiplying all random processes are null. On the other hand, we can regroup the following terms:

$$\begin{aligned}
\frac{\boldsymbol{\Sigma}_{3,.}\boldsymbol{\Sigma}_{3,.}^\top}{2}\left(\sum_{k=1}^{n}\left(\frac{c}{\Gamma(\alpha)}m_k-d_k\right)\right)^2&=\frac{1}{2}\frac{\left(\sum_{l=1}^{n}m_l\right)^2\boldsymbol{\Sigma}_{3,.}\boldsymbol{\Sigma}_{3,.}^\top}{\Gamma(\alpha)^2}c^2\\
-\frac{\boldsymbol{\Sigma}_{3,.}\boldsymbol{\Sigma}_{3,.}^\top\left(\sum_{l=1}^{n}m_l\right)}{\Gamma(\alpha)}\sum_{k=1}^{n}cd_k&+\frac{1}{2}\boldsymbol{\Sigma}_{3,.}\boldsymbol{\Sigma}_{3,.}^\top\sum_{k_1=1,k_2=1}^{n}d_{k_1}d_{k_2}\,.
\end{aligned}$$

We infer that functions $a(t,s)$, $c(t,s)$ and $d_k(t,s)$ solves a system of ordinary differential equations:

$$\begin{aligned}
\partial_t a &= -\boldsymbol{\omega}^\top \left(\boldsymbol{r} - \boldsymbol{\lambda} \odot (\boldsymbol{\varphi}(1) - 1)\right) - \boldsymbol{\lambda}^\top \left(\boldsymbol{\varphi}(\boldsymbol{\omega}) - 1\right) \\
&\quad -\kappa\theta \sum_{k=1}^{n} \left(\frac{c}{\Gamma(\alpha)} m_k - d_k\right), \\
\partial_t c &= \frac{1}{2}\boldsymbol{\omega}^\top diag(\boldsymbol{\Sigma}_{1:2,.}\boldsymbol{\Sigma}_{1:2,.}^\top) - \frac{1}{2}\boldsymbol{\omega}^\top \left(\boldsymbol{\Sigma}_{1:2,.}\boldsymbol{\Sigma}_{1:2,.}^\top\right)\boldsymbol{\omega} \\
&\quad -\frac{\boldsymbol{\Sigma}_{3,.}\boldsymbol{\Sigma}_{3,.}^\top}{2}\left(\sum_{k=1}^{n}\left(\frac{c}{\Gamma(\alpha)} m_k - d_k\right)\right)^2 \\
&\quad + \left(\kappa - \boldsymbol{\omega}^\top \boldsymbol{\Sigma}_{1:2,.}\boldsymbol{\Sigma}_{3,.}^\top\right)\sum_{k=1}^{n}\left(\frac{c}{\Gamma(\alpha)} m_k - d_k\right), \\
\partial_t d_k &= -\left(\frac{c}{\Gamma(\alpha)} m_k - d_k\right) b_k .
\end{aligned}$$

From this last equation, we check that $d_k(t,s)$ is given by (25) and that $a(.)$ and $c(.)$ solve Equations (26), (27).

■

In the same manner, we find the joint characteristic function of log-returns under the $\mathbb{S}$-measure. We provide then the result in the next proposition without proof.

**Proposition 5.2.** *For $\boldsymbol{\omega} = (\omega_1, \omega_2)^\top \in \mathbb{C}^{2,-}$ and $0 \le t \le s$, the characteristic function of log-returns $\bar{\boldsymbol{X}}_s = (\bar{X}_s^{(1)}, \bar{X}_s^{(2)})$ under the $\mathbb{S}$ measure is*

$$\mathbb{E}^{\mathbb{S}}\left(e^{\boldsymbol{\omega}^\top \bar{\boldsymbol{X}}_s} | \mathcal{F}_t\right) = \exp\left(a^{\mathbb{S}}(t,s) + c^{\mathbb{S}}(t,s)\bar{V}_t - \sum_{k=1}^{n} d_k(t,s) Y_t^{(k)} + \boldsymbol{\omega}^\top \bar{\boldsymbol{X}}_t\right), \tag{30}$$

*where $d_k(t,s)$ is defined by Equation (25). If we note $\lambda_1^{\mathbb{S}} = \lambda_1 \varphi^{(1)}(1)$ , $\kappa^{\mathbb{S}} = \kappa - \boldsymbol{\Sigma}_{3,.}\boldsymbol{\Sigma}_{1:2,.}^\top \boldsymbol{e}_1$ and*

$$h_k^{\mathbb{S}}(t,s) \;=\; c^{\mathbb{S}}(t,s) - b_k \int_t^s e^{-b_k(u-t)} c^{\mathbb{S}}(u,s) du ,$$

*functions $a^{\mathbb{S}}(t,s)$ and $c^{\mathbb{S}}(t,s)$ solve a system of ODE's:*

$$\partial_t a^{\mathbb{S}}(t,s) = -\boldsymbol{\omega}^\top \left(\boldsymbol{r} - \boldsymbol{\lambda} \odot (\boldsymbol{\varphi}(1) - 1)\right) - \boldsymbol{\lambda}^{\mathbb{S}\top}\left(\boldsymbol{\varphi}^{\mathbb{S}}(\boldsymbol{\omega}) - 1\right) - \kappa\theta \sum_{k=1}^{n} \frac{m_k h_k^{\mathbb{S}}(t,s)}{\Gamma(\alpha)}, \tag{31}$$

$$\begin{aligned}
\partial_t c^{\mathbb{S}}(t,s) &= -\boldsymbol{\omega}^\top \left(\boldsymbol{\Sigma}_{1:2,.}\boldsymbol{\Sigma}_{1:2,.}^\top \boldsymbol{e}_1 - \frac{1}{2} diag(\boldsymbol{\Sigma}_{1:2,.}\boldsymbol{\Sigma}_{1:2,.}^\top)\right) - \frac{1}{2}\boldsymbol{\omega}^\top \left(\boldsymbol{\Sigma}_{1:2,.}\boldsymbol{\Sigma}_{1:2,.}^\top\right)\boldsymbol{\omega} \qquad (32) \\
&\quad + \left(\kappa^{\mathbb{S}} - \boldsymbol{\omega}^\top \boldsymbol{\Sigma}_{1:2,.}\boldsymbol{\Sigma}_{3,.}^\top\right)\sum_{k=1}^{n}\frac{m_k h_k^{\mathbb{S}}(t,s)}{\Gamma(\alpha)} - \frac{\boldsymbol{\Sigma}_{3,.}\boldsymbol{\Sigma}_{3,.}^\top}{2}\left(\sum_{k=1}^{n}\frac{m_k h_k^{\mathbb{S}}(t,s)}{\Gamma(\alpha)}\right)^2 .
\end{aligned}$$

*with the terminal conditions $a(s,s) = 0$ and $c(s,s) = 0$.*

Propositions 9.1 and 9.2 in Appendix B, provide the characteristic functions of log-returns when the variance is ruled by a CIR, as defined by Equation (7). A comparison with propositions 5.1 and 5.2 emphasizes the similarities between the rough and non-rough models. We infer in the next corollary that $c(t,s)$ and $c^{\mathbb{S}}(t,s)$ are homogeneous in the sense they only depend on $(s-t)$. This property is used later to study the limit case when $n \to \infty$,which corresponds to the initial model.

**Corollary 5.3.** *For any $s, s' \in \mathbb{R}^+$ and $v \in \mathbb{R}^+$, the following equality holds*

$$c(s-v,s) = c(s'-v,s')\,, \tag{33}$$

$$c^{\mathbb{S}}(s-v,s) = c^{\mathbb{S}}(s'-v,s')\,. \tag{34}$$

**Proof** By definition the equality (33) is true for $v=0$, $c(s,s)=c(s',s')=0$. Let us then assume that the property (33) holds for all $l \in [0,v]$ where $0 < v \le s$. From Equations (27) and (25), we notice that

$$\begin{aligned} \frac{\partial c(s-v,s)}{\partial v} &= -\left.\frac{\partial c(t,s)}{\partial t}\right|_{t=s-v} = \frac{1}{2}\boldsymbol{\omega}^\top diag(\boldsymbol{\Sigma}_{1:2,.}\boldsymbol{\Sigma}_{1:2,.}^\top) - \frac{1}{2}\boldsymbol{\omega}^\top\left(\boldsymbol{\Sigma}_{1:2,.}\boldsymbol{\Sigma}_{1:2,.}^\top\right)\boldsymbol{\omega} \\ &+ \frac{\boldsymbol{\Sigma}_{3,.}\boldsymbol{\Sigma}_{3,.}^\top}{2}\left(\sum_{k=1}^{n}\frac{m_k}{\Gamma(\alpha)}\left(c(s-v,s) - b_k\int_{s-v}^{s} e^{-b_k(u-(s-v))}c(u,s)du\right)\right)^2 \\ &- \left(\kappa - \boldsymbol{\omega}^\top\boldsymbol{\Sigma}_{1:2,.}\boldsymbol{\Sigma}_{3,.}^\top\right)\sum_{k=1}^{n}\frac{m_k}{\Gamma(\alpha)}\left(c(s-v,s) - b_k\int_{s-v}^{s} e^{-b_k(u-(s-v))}c(u,s)du\right)\,. \end{aligned}$$

We rewrite the integrals in the previous equation using the change of variable $u = s-l$,

$$\int_{s-v}^{s} e^{-b_k(u-(s-v))}c(u,s)\,du = \int_0^v e^{-b_k(v-l)}c(s-l,s)\,dl\,.$$

Since $c(s-l,s) = c(s'-l,s')$ for all $l \in [0,v]$, we infer that

$$\frac{\partial c(s-v,s)}{\partial v} = \frac{\partial c(s'-v,s')}{\partial v}\,,$$

and conclude that the equality (33) also holds for $v+dv$. The proof of Equation (34) is similar.

■

A natural way to find the characteristic function of log-returns under $\mathbb{Q}$ or $\mathbb{S}$ in the initial model, is to consider the limit of systems in Propositions 5.1 or 5.2 when the granularity of the partition tends to infinity. Nevertheless, this approach fails because the limit of the sum of $m_k$ is not defined:

$$\lim_{n\to\infty}\sum_{k=1}^{n} m_k = \int_0^\infty \gamma(d\xi) = \infty\,.$$

In order to find the limit of characteristic functions when $n \to \infty$, we first prove that they are computable in the finite dimensional model by solving a system of forward differential equations. Next, we will show that the limit of this system is a function of Riemann-Liouville derivatives.

**Proposition 5.4.** *For $\omega \in \mathbb{C}^{2,-}$ and $0 \le t \le s$, the characteristic function of stock log-returns is given by*

$$\mathbb{E}\left(e^{\boldsymbol{\omega}^\top \bar{\boldsymbol{X}}_s} | \mathcal{F}_t\right) = \exp\left(a(t,s) + c(t,s)\bar{V}_t - \sum_{k=1}^{n} d_k(t,s) Y_t^{(k)} + \boldsymbol{\omega}^\top \bar{\boldsymbol{X}}_t\right). \tag{35}$$

*where $d_k(t,s)$ is given by Equation (25) and functions $a(0,s)$ and $c(0,s)$ solves forward ODE's:*

$$\partial_s a(t,s) = \boldsymbol{\omega}^\top \left(\boldsymbol{r} - \boldsymbol{\lambda} \odot (\boldsymbol{\varphi}(1) - 1)\right) + \boldsymbol{\lambda}^\top \left(\boldsymbol{\varphi}(\boldsymbol{\omega}) - 1\right) + \frac{\kappa\theta}{\Gamma(\alpha)} \sum_{k=1}^{n} m_k \left(\partial_s \int_t^s e^{-b_k(v-t)} c(v,s)\, dv\right), \tag{36}$$

$$\begin{aligned}\partial_s c(t,s) = &-\frac{1}{2}\boldsymbol{\omega}^\top diag(\boldsymbol{\Sigma}_{1:2,.}\boldsymbol{\Sigma}_{1:2,.}^\top) + \frac{1}{2}\boldsymbol{\omega}^\top \left(\boldsymbol{\Sigma}_{1:2,.}\boldsymbol{\Sigma}_{1:2,.}^\top\right)\boldsymbol{\omega} \\ &+ \frac{\boldsymbol{\Sigma}_{3,.}\boldsymbol{\Sigma}_{3,.}^\top}{2\,\Gamma(\alpha)^2}\partial_s \int_t^s \left(\sum_{k=1}^{n} m_k \left(\partial_s \int_t^s e^{-b_k(v-t)} c(v,s)\, dv\right)\right)^2 dv \\ &- \left(\kappa - \boldsymbol{\omega}^\top \boldsymbol{\Sigma}_{1:2,.}\boldsymbol{\Sigma}_{3,.}^\top\right) \sum_{k=1}^{n} m_k \left(\partial_s \int_t^s e^{-b_k(v-t)} c(v,s)\, dv\right).\end{aligned} \tag{37}$$

*with the initial conditions $a(0,0) = 0$ and $c(0,0) = 0$.*

**Proof** We momentarily note $a_0(\boldsymbol{\omega}) = \boldsymbol{\omega}^\top \left(\boldsymbol{r} - \boldsymbol{\lambda} \odot (\boldsymbol{\varphi}(1) - 1)\right) + \boldsymbol{\lambda}^\top \left(\boldsymbol{\varphi}(\boldsymbol{\omega}) - 1\right)$. From Proposition 5.1 and given that $a(s,s) = 0$, we infer that

$$\begin{aligned} a(t,s) &= a_0(\boldsymbol{\omega})(s-t) + \frac{\kappa\theta}{\Gamma(\alpha)} \sum_{k=1}^{n} m_k \left(\int_t^s c(u,s) du - b_k \int_t^s \int_u^s e^{-b_k(v-u)} c(v,s) dv\, du\right) \\ &= a_0(\boldsymbol{\omega})(s-t) + \frac{\kappa\theta}{\Gamma(\alpha)} \sum_{k=1}^{n} m_k \left(\int_t^s c(u,s) du - b_k \int_t^s \frac{1}{b_k}\left(1 - e^{-b_k(v-t)}\right) c(v,s)\, dv\right) \\ &= a_0(\boldsymbol{\omega})(s-t) + \frac{\kappa\theta}{\Gamma(\alpha)} \sum_{k=1}^{n} m_k \left(\int_t^s e^{-b_k(v-t)} c(v,s)\, dv\right). \end{aligned}$$

Deriving this last equation with respect to $s$ allows us to obtain Equation (36). Let us note $c_0(\boldsymbol{\omega}) = -\frac{1}{2}\boldsymbol{\omega}^\top diag(\boldsymbol{\Sigma}_{1:2,.}\boldsymbol{\Sigma}_{1:2,.}^\top) + \frac{1}{2}\boldsymbol{\omega}^\top \left(\boldsymbol{\Sigma}_{1:2,.}\boldsymbol{\Sigma}_{1:2,.}^\top\right)\boldsymbol{\omega}$. From Proposition 5.1 and as $c(s,s) = 0$, we obtain an integral representation of $c(t,s)$,

$$\begin{aligned} c(t,s) \;=\; & c_0(\boldsymbol{\omega})(s-t) + \frac{\boldsymbol{\Sigma}_{3,.}\boldsymbol{\Sigma}_{3,.}^\top}{2\,\Gamma(\alpha)^2} \int_t^s \left(\sum_{k=1}^{n} m_k \left(c(v,s) - b_k \int_v^s e^{-b_k(u-v)} c(u,s)\, du\right)\right)^2 dv \\ & - \left(\kappa - \boldsymbol{\omega}^\top \boldsymbol{\Sigma}_{1:2,.}\boldsymbol{\Sigma}_{3,.}^\top\right) \sum_{k=1}^{n} m_k \left(\int_t^s e^{-b_k(v-t)} c(v,s)\, dv\right). \end{aligned}$$

Deriving this last expression with respect to $s$ leads to

$$\partial_s c(t,s) = \frac{\boldsymbol{\Sigma}_{3,.}\boldsymbol{\Sigma}_{3,.}^\top}{2\,\Gamma(\alpha)^2}\partial_s \int_t^s \left(\sum_{k=1}^n m_k \left(c(v,s) - b_k \int_v^s e^{-b_k(u-v)} c(u,s)\,du\right)\right)^2 dv \tag{38}$$
$$- \left(\kappa - \boldsymbol{\omega}^\top \boldsymbol{\Sigma}_{1:2,.}\boldsymbol{\Sigma}_{3,.}^\top\right) \sum_{k=1}^n m_k \left(\partial_s \int_t^s e^{-b_k(v-t)}\, c(v,s)\,dv\right) + c_0(\boldsymbol{\omega})\,,$$

where the derivative in the first term of this equation is developped as the following sum:

$$\frac{1}{2}\partial_s \int_t^s \left(\sum_{k=1}^n m_k \left(c(v,s) - b_k \int_v^s e^{-b_k(u-v)} c(u,s)du\right)\right)^2 dv \tag{39}$$
$$= \sum_{k=1}^n \sum_{l=1}^n m_k m_l \int_t^s \left(c(v,s)\partial_s c(v,s)\right) dv$$
$$- \sum_{k=1}^n \sum_{l=1}^n m_k m_l b_l \int_t^s \left(c(v,s) \int_v^s e^{-b_l(u-v)} \partial_s c(u,s)du\right) dv$$
$$- \sum_{k=1}^n \sum_{l=1}^n m_k m_l b_k \int_t^s \left(\partial_s c(v,s) \int_v^s e^{-b_k(u-v)} c(u,s)du\right) dv$$
$$+ \sum_{k=1}^n \sum_{l=1}^n m_k m_l b_k b_l \int_t^s \left(\int_v^s e^{-b_k(u-v)} c(u,s)du \int_v^s e^{-b_l(u-v)} \partial_s c(u,s)du\right) dv\,.$$

As $c(v,s)\partial_s c(v,s) = \frac{1}{2}\partial_s c(v,s)^2$, the first term in this last equation is rewritten as

$$\int_t^s \left(c(v,s)\partial_s c(v,s)\right) dv = \frac{1}{2}\partial_s \int_t^s c(v,s)^2 dv\,.$$

On the other hand, the sum of the second and third terms in Equation (39) are gathered as follows:

$$\sum_{k=1}^n \sum_{l=1}^n m_k m_l b_l \int_t^s \left(c(v,s) \int_v^s e^{-b_l(u-v)} \partial_s c(u,s)du\right) dv +$$
$$\sum_{k=1}^n \sum_{l=1}^n m_k m_l b_k \int_t^s \left(\partial_s c(v,s) \int_v^s e^{-b_k(u-v)} c(u,s)du\right) dv$$
$$= \sum_{k=1}^n \sum_{l=1}^n m_k m_l\, b_k \partial_s \int_t^s \left(c(v,s) \int_v^s e^{-b_k(u-v)} c(u,s)du\right) dv\,.$$

As $\partial_s \int_v^s e^{-b_l(u-v)} c(u,s)du = \int_v^s e^{-b_l(u-v)} \partial_s c(u,s)du$, we rewrite the last term of Equation (39) as follows:

$$\sum_{k=1}^n \sum_{l=1}^n m_k m_l b_k b_l \int_t^s \left(\int_v^s e^{-b_k(u-v)} c(u,s)du \int_v^s e^{-b_l(u-v)} \partial_s c(u,s)du\right) dv =$$
$$\frac{1}{2}\sum_{k=1}^n \sum_{l=1}^n m_k m_l b_k b_l \partial_s \int_t^s \left(\int_v^s e^{-b_k(u-v)} c(u,s)du \int_v^s e^{-b_l(u-v)} c(u,s)du\right) dv\,.$$

We finally obtain that

$$
\begin{aligned}
&\frac{1}{2}\partial_s \int_t^s \left(\sum_{k=1}^n m_k \left(c(v,s) - b_k \int_v^s e^{-b_k(u-v)} c(u,s) du\right)\right)^2 dv \\
&= \frac{1}{2}\left(\sum_{k=1}^n m_k \partial_s \int_t^s \left(c(v,s) - b_k \int_v^s e^{-b_k(u-v)} c(u,s) du\right) dv\right)^2 \\
&= \frac{1}{2}\left(\sum_{k=1}^n m_k \partial_s \int_t^s e^{-b_k(u-t)}\, c(u,s)\, du\right)^2 .
\end{aligned} \tag{40}
$$

Injecting this result into Equation (38) leads to the expression (37).

■

A similar approach is used to retrieve the forward equations satisfied by functions $a^{\mathbb{S}}(t,s)$ and $c^{\mathbb{S}}(t,s)$ involved in the definition of the characteristic function (30) of log-returns under the $\mathbb{S}$ measure. For this reason, the result is provided without proof.

**Proposition 5.5.** *For $\omega \in \mathbb{C}^{2,-}$ and $0 \leq t \leq s$, the characteristic function of stock log-returns under the measure $\mathbb{S}$ is given by*

$$
\mathbb{E}^{\mathbb{S}}\left(e^{\boldsymbol{\omega}^\top \bar{\boldsymbol{X}}_s} | \mathcal{F}_t\right) = \exp\left(a^{\mathbb{S}}(t,s) + c^{\mathbb{S}}(t,s)\bar{V}_t - \sum_{k=1}^n d_k(t,s) Y_t^{(k)} + \boldsymbol{\omega}^\top \bar{\boldsymbol{X}}_t\right) \tag{41}
$$

*where $d_k(t,s)$ is given by Equation (25) and functions $a^{\mathbb{S}}(0,s)$ and $c^{\mathbb{S}}(0,s)$ solves a forward system of ordinary differential equations:*

$$
\begin{aligned}
\partial_s a^{\mathbb{S}}(t,s) &= \boldsymbol{\omega}^\top \left(\boldsymbol{r} - \boldsymbol{\lambda} \odot (\boldsymbol{\varphi}(1) - 1)\right) + \boldsymbol{\lambda}^{\mathbb{S}\top}\left(\boldsymbol{\varphi}^{\mathbb{S}}(\boldsymbol{\omega}) - 1\right) \qquad (42)\\
&\quad + \frac{\kappa\theta}{\Gamma(\alpha)} \sum_{k=1}^n m_k \left(\partial_s \int_t^s e^{-b_k(v-t)}\, c^{\mathbb{S}}(v,s)\, dv\right), \\
\partial_s c^{\mathbb{S}}(t,s) &= \boldsymbol{\omega}^\top \left(\boldsymbol{\Sigma}_{1:2,.}\boldsymbol{\Sigma}_{1:2,.}^\top \boldsymbol{e}_1 - \frac{1}{2} diag(\boldsymbol{\Sigma}_{1:2,.}\boldsymbol{\Sigma}_{1:2,.}^\top)\right) + \frac{1}{2}\boldsymbol{\omega}^\top \left(\boldsymbol{\Sigma}_{1:2,.}\boldsymbol{\Sigma}_{1:2,.}^\top\right)\boldsymbol{\omega} \qquad (43)\\
&\quad + \frac{\boldsymbol{\Sigma}_{3,.}\boldsymbol{\Sigma}_{3,.}^\top}{2\,\Gamma(\alpha)^2}\partial_s \int_t^s \left(\sum_{k=1}^n m_k \left(\partial_s \int_t^s e^{-b_k(v-t)}\, c^{\mathbb{S}}(v,s)\, dv\right)\right)^2 dv \\
&\quad - \left(\kappa^{\mathbb{S}} - \boldsymbol{\omega}^\top \boldsymbol{\Sigma}_{1:2,.}\boldsymbol{\Sigma}_{3,.}^\top\right) \sum_{k=1}^n m_k \left(\partial_s \int_t^s e^{-b_k(v-t)}\, c^{\mathbb{S}}(v,s)\, dv\right).
\end{aligned}
$$

*with the initial conditions $a(0,0) = 0$ and $c(0,0) = 0$.*

Propositions 5.4 and 5.5 are key results to infer the characteristic functions of log-returns in the original model.

# 6 Characteristic function of log-returns in the infinite dimensional model

We study in this section the limit of equations (36) and (37) in order to infer the characteristic function of log-returns in the initial market model of Section 2. Let us recall that the left Riemann-Liouville integral for $\alpha \in (0,1]$ is defined for any integrable functions $f(.)$ as follows:

$$I^{\alpha} f(t) = \frac{1}{\Gamma(\alpha)} \int_0^t (t-u)^{\alpha-1} f(u)\, du \, .$$

By construction, $I^{\alpha} f(t)$ corresponds to the classical Riemann integral when $\alpha = 1$. The left Riemann-Liouville derivative, denoted by $D^{1-\alpha} f(t)$, is the derivative of $I^{\alpha} f(t)$:

$$D^{1-\alpha} f(t) = \frac{d I^{\alpha} f(t)}{dt} = \frac{1}{\Gamma(\alpha)} \frac{d}{dt} \int_0^t \frac{f(u)}{(t-u)^{1-\alpha}}\, du \, .$$

If we remember that $(t-u)^{\alpha-1}$ is also an integral with respect to a measure $\gamma(d\xi)$:

$$(t-u)^{\alpha-1} = \frac{1}{\Gamma(1-\alpha)} \int_0^{\infty} \frac{e^{-(t-u)\xi}}{\xi^{\alpha}} d\xi := \int_0^{\infty} e^{-(t-u)\xi} \gamma(d\xi) \, ,$$

the left fractional derivative is also an integral with respect to this measure:

$$\begin{aligned}
D^{1-\alpha} f(t) &= \frac{1}{\Gamma(\alpha)} \frac{d}{dt} \int_0^t \frac{f(u)}{(t-u)^{1-\alpha}}\, du \\
&= \frac{1}{\Gamma(\alpha)} \int_0^{\infty} \frac{d}{dt} \int_0^t \frac{e^{-(t-u)\xi}}{\Gamma(1-\alpha)\xi^{\alpha}} f(u)\, du\, d\xi \\
&= \frac{1}{\Gamma(\alpha)} \int_0^{\infty} \left( f(t) - \xi \int_0^t e^{-(t-u)\xi} f(u)\, du \right) \gamma(d\xi) \\
&= \frac{1}{\Gamma(\alpha)} \int_0^{\infty} \left( \frac{d}{dt} \int_0^t e^{-(t-u)\xi} f(u)\, du \right) \gamma(d\xi)
\end{aligned}$$

If we replace the measure $\gamma(.)$ by its discrete equivalent $\bar{\gamma}(.)$ on a partition $\mathcal{E}^{(n)}$, as defined by equations (13) and (14), the fractional derivative is then approached by :

$$D^{1-\alpha,(n)} f(t) = \frac{1}{\Gamma(\alpha)} \sum_{k=0}^{n} m_k \left( \frac{d}{dt} \int_0^t e^{-(t-u)b_k} f(u)\, du \right) . \tag{44}$$

If we compare this last expression with equations (36) and (37), we recognize similar patterns. This conclusion is the starting point of the proof of the next result.

**Proposition 6.1.** *Let us denote by $\psi(s)$, the solution of the fractional forward ODE:*

$$\begin{aligned}
D^{\alpha}\psi(s) = &-\frac{1}{2}\boldsymbol{\omega}^{\top} diag(\boldsymbol{\Sigma}_{1:2,.}\boldsymbol{\Sigma}_{1:2,.}^{\top}) + \frac{1}{2}\boldsymbol{\omega}^{\top}\left(\boldsymbol{\Sigma}_{1:2,.}\boldsymbol{\Sigma}_{1:2,.}^{\top}\right)\boldsymbol{\omega} \\
&- \left(\kappa - \boldsymbol{\omega}^{\top}\boldsymbol{\Sigma}_{1:2,.}\boldsymbol{\Sigma}_{3,.}^{\top}\right)\psi(s) + \frac{\boldsymbol{\Sigma}_{3,.}\boldsymbol{\Sigma}_{3,.}^{\top}}{2}\psi(s)^2 \, ,
\end{aligned} \tag{45}$$

*with the initial condition $\psi(0) = 0$. The characteristic function of $\boldsymbol{X}_s$, conditionally to the filtration at time $t = 0$ is*

$$\mathbb{E}\left(e^{\boldsymbol{\omega}^\top \boldsymbol{X}_s} | \mathcal{F}_0\right) = \exp\left(a(0,s) + c(0,s)V_t\right) , \tag{46}$$

*where $c(0,s) = I^{1-\alpha}\psi(s)$ and $a(0,s)$ solves the forward ordinary differential equation*

$$\partial_s a(0,s) = \boldsymbol{\omega}^\top \left(\boldsymbol{r} - \boldsymbol{\lambda} \odot (\boldsymbol{\varphi}(1) - 1)\right) + \boldsymbol{\lambda}^\top \left(\boldsymbol{\varphi}(\boldsymbol{\omega}) - 1\right) + \kappa\theta\, \psi(s) , \tag{47}$$

*with the initial condition $a(0,0) = 0$.*

**Proof** From property (33), $c(t,s)$ is an homogeneous function of $v = (s-t)$. We denote it by $\tilde{c}(v) = c(s-v, s)$. If we perform the change of variable $v = s - u$, we have that

$$\int_0^s e^{-b_k u} c(u,s)\, du \quad = \quad \int_0^s e^{-b_k (s-v)} \tilde{c}(v)\, dv ,$$

and we retrieve in the left term of Equation (36), the discretized fractional derivative of $\tilde{c}(.)$:

$$\frac{1}{\Gamma(\alpha)} \sum_{k=1}^{n} m_k \partial_s \int_0^s e^{-b_k u}\, c(u,s)\, du = D^{1-\alpha,(n)} \tilde{c}(s) .$$

The derivative of the function $a(0,s)$ depends upon this discretized fractional derivative,

$$\begin{aligned} \partial_s a_j(0,s) \quad &= \quad \boldsymbol{\omega}^\top \left(\boldsymbol{r} - \boldsymbol{\lambda} \odot (\boldsymbol{\varphi}(1) - 1)\right) + \boldsymbol{\lambda}^\top \left(\boldsymbol{\varphi}(\boldsymbol{\omega}) - 1\right) \\ & \quad\quad + \kappa\, \theta\, \left(D^{1-\alpha,(n)} \tilde{c}(s)\right) . \end{aligned} \tag{48}$$

In a similar manner, the derivative of $c_j(0,s)$ with respect to the considered time horizon becomes:

$$\begin{aligned} \partial_s c(0,s) = & -\frac{1}{2}\boldsymbol{\omega}^\top diag(\boldsymbol{\Sigma}_{1:2,.} \boldsymbol{\Sigma}_{1:2,.}^\top) + \frac{1}{2}\boldsymbol{\omega}^\top \left(\boldsymbol{\Sigma}_{1:2,.} \boldsymbol{\Sigma}_{1:2,.}^\top\right) \boldsymbol{\omega} \\ & - \left(\kappa - \boldsymbol{\omega}^\top \boldsymbol{\Sigma}_{1:2,.} \boldsymbol{\Sigma}_{3,.}^\top\right) \left(D^{1-\alpha,(n)} \tilde{c}(s)\right) + \frac{\boldsymbol{\Sigma}_{3,.} \boldsymbol{\Sigma}_{3,.}^\top}{2} \left(D^{1-\alpha,(n)} \tilde{c}(s)\right)^2 . \end{aligned} \tag{49}$$

When the size of the partition $\mathcal{E}^{(n)}$ growths to infinity, the limit of Equations (48) and (49) are given by:

$$\begin{aligned} \partial_s a(0,s) \quad &= \quad \boldsymbol{\omega}^\top \left(\boldsymbol{r} - \boldsymbol{\lambda} \odot (\boldsymbol{\varphi}(1) - 1)\right) + \boldsymbol{\lambda}^\top \left(\boldsymbol{\varphi}(\boldsymbol{\omega}) - 1\right) + \kappa\theta \left(D^{1-\alpha} \tilde{c}(s)\right) , \\ \partial_s c(0,s) \quad &= \quad -\frac{1}{2}\boldsymbol{\omega}^\top diag(\boldsymbol{\Sigma}_{1:2,.} \boldsymbol{\Sigma}_{1:2,.}^\top) + \frac{1}{2}\boldsymbol{\omega}^\top \left(\boldsymbol{\Sigma}_{1:2,.} \boldsymbol{\Sigma}_{1:2,.}^\top\right) \boldsymbol{\omega} \\ & \quad\quad - \left(\kappa - \boldsymbol{\omega}^\top \boldsymbol{\Sigma}_{1:2,.} \boldsymbol{\Sigma}_{3,.}^\top\right) \left(D^{1-\alpha} \tilde{c}(s)\right) + \frac{\boldsymbol{\Sigma}_{3,.} \boldsymbol{\Sigma}_{3,.}^\top}{2} \left(D^{1-\alpha} \tilde{c}(s)\right)^2 . \end{aligned}$$

Let us denote $\psi(s) = D^{1-\alpha}\tilde{c}(s)$. By definition of the fractional integral, this is the inverse operator of the fractional derivative, i.e. $I^{1-\alpha} D^{1-\alpha} f(t) = f(t)$. The function $c(0,s)$ is then equal to $c(0,s) = I^{1-\alpha}\psi(s) = \tilde{c}(s)$. By definition of the left Riemann-Liouville derivative, we finally infer that

$$\partial_s c(0,s) \;=\; \frac{dI^{1-\alpha}\psi(s)}{ds} = D^{\alpha}\psi(s)\,.$$

This last relation allows us to obtain Equations (45) and (47).

■

Similar arguments allow us to find the characteristic function of log-returns under the $\mathbb{S}$ measure.

**Proposition 6.2.** *Let us denote by $\psi^{\mathbb{S}}(s)$, the solution of the fractional forward ODE:*

$$\begin{aligned} D^{\alpha}\psi^{\mathbb{S}}(s) &= \boldsymbol{\omega}^{\top}\left(\boldsymbol{\Sigma}_{1:2,.}\boldsymbol{\Sigma}_{1:2,.}^{\top}\boldsymbol{e}_1 - \frac{1}{2}diag(\boldsymbol{\Sigma}_{1:2,.}\boldsymbol{\Sigma}_{1:2,.}^{\top})\right) + \frac{1}{2}\boldsymbol{\omega}^{\top}\left(\boldsymbol{\Sigma}_{1:2,.}\boldsymbol{\Sigma}_{1:2,.}^{\top}\right)\boldsymbol{\omega} \\ &\quad - \left(\kappa^{\mathbb{S}} - \boldsymbol{\omega}^{\top}\boldsymbol{\Sigma}_{1:2,.}\boldsymbol{\Sigma}_{3,.}^{\top}\right)\psi^{\mathbb{S}} + \frac{\boldsymbol{\Sigma}_{3,.}\boldsymbol{\Sigma}_{3,.}^{\top}}{2}\left(\psi^{\mathbb{S}}\right)^2 , \end{aligned} \tag{50}$$

*with the initial condition $\psi^{\mathbb{S}}(0) = 0$. The characteristic function of $\boldsymbol{X}_s$ under the $\mathbb{S}$ measure, conditionally to the filtration at time $t = 0$ is*

$$\mathbb{E}^{\mathbb{S}}\left(e^{\boldsymbol{\omega}^{\top}\boldsymbol{X}_s}|\mathcal{F}_0\right) = \exp\left(a^{\mathbb{S}}(0,s) + c^{\mathbb{S}}(0,s)V_t\right)\,, \tag{51}$$

*where $c^{\mathbb{S}}(0,s) = I^{1-\alpha}\psi^{\mathbb{S}}(s)$ and $a^{\mathbb{S}}(0,s)$ solves the forward ordinary differential equation*

$$\partial_s a^{\mathbb{S}}(0,s) = \boldsymbol{\omega}^{\top}\left(\boldsymbol{r} - \boldsymbol{\lambda}\odot(\boldsymbol{\varphi}(1) - 1)\right) + \boldsymbol{\lambda}^{\mathbb{S}\top}\left(\boldsymbol{\varphi}^{\mathbb{S}}(\boldsymbol{\omega}) - 1\right) + \kappa\theta\,\psi^{\mathbb{S}}(s)\,, \tag{52}$$

*with the initial condition $a^{\mathbb{S}}(0,0) = 0$.*

In numerical applications, we may think to compute the characteristic function with the finite dimensional approximation proposed in Propositions 5.1, 5.2, 5.4 or 5.5. Nevertheless, this approach implies solving PDE's for $a(.,.)$ and $c(.,.)$ (or $a^{\mathbb{S}}(.,.)$ and $c^{\mathbb{S}}(.,.)$) , that are functions of sum of $m_k$ tending to infinity when the granularity of the partition $\mathcal{E}^{(n)}$ increases. This can cause numerical instabilities that makes difficult the computations of the characteristic function. A more reliable method consists to calculate the functions $\psi(t)$, $c(0,t)$ and $a(0,t)$ (resp. $\psi^{\mathbb{S}}(t)$, $c^{\mathbb{S}}(0,t)$ and $a^{\mathbb{S}}(0,t)$) such as defined in Proposition 6.1 (resp. 6.2). Let us denote

$$\psi_0(\boldsymbol{\omega}) = \frac{1}{2}\boldsymbol{\omega}^{\top}\left(\boldsymbol{\Sigma}_{1:2,.}\boldsymbol{\Sigma}_{1:2,.}^{\top}\right)\boldsymbol{\omega} - \frac{1}{2}\boldsymbol{\omega}^{\top}diag(\boldsymbol{\Sigma}_{1:2,.}\boldsymbol{\Sigma}_{1:2,.}^{\top})\,.$$

Since $D_0^{\alpha}I_0^{\alpha}f(t) = f(t)$, the fractional integral of Equation (45) provides us the following expression for $\psi$ ,

$$\psi(t) \;=\; \int_0^t \frac{(t-s)^{\alpha_j - 1}}{\Gamma(\alpha_j)}\left(\psi_0(\boldsymbol{\omega}) - \left(\kappa - \boldsymbol{\omega}^{\top}\boldsymbol{\Sigma}_{1:2,.}\boldsymbol{\Sigma}_{3,.}^{\top}\right)\psi(s) + \frac{\boldsymbol{\Sigma}_{3,.}\boldsymbol{\Sigma}_{3,.}^{\top}}{2}\psi(s)^2\right)ds$$

that we discretize. We choose a time step, $\Delta$ and denote $t_k = k\,\Delta$ for $k = 0, ...., n_t$ where $n_t = \left\lfloor \frac{t}{\Delta} \right\rfloor$. To ligthen developments, we denote by $\psi(k)$ the approached value of $\psi$ at time $t_k$, computed with the recursion50

$$\psi(k) = \sum_{l=0}^{k-1} \frac{\left((t_k - t_l)^{\alpha_j} - (t_k - t_{l+1})^{\alpha_j}\right)}{\alpha_j \Gamma(\alpha_j)} \Big(\psi_0(\boldsymbol{\omega}) - \left(\kappa - \boldsymbol{\omega}^\top \boldsymbol{\Sigma}_{1:2,.} \boldsymbol{\Sigma}_{3,.}^\top\right) \psi(l) + \frac{\boldsymbol{\Sigma}_{3,.} \boldsymbol{\Sigma}_{3,.}^\top}{2} \psi(l)^2 \Big) , \tag{53}$$

for $k = 1, ...., n_t$ and an initial value $\psi(0) = 0$. In a similar manner, the approached value of $\psi^{\mathbb{S}}$ is computed by

$$\psi^{\mathbb{S}}(k) = \sum_{l=0}^{k-1} \frac{\left((t_k - t_l)^{\alpha_j} - (t_k - t_{l+1})^{\alpha_j}\right)}{\alpha_j \Gamma(\alpha_j)} \Big(\psi_0(\boldsymbol{\omega}) + \boldsymbol{\omega}^\top \boldsymbol{\Sigma}_{1:2,.} \boldsymbol{\Sigma}_{1:2,.}^\top \boldsymbol{e}_1 - \left(\kappa^{\mathbb{S}} - \boldsymbol{\omega}^\top \boldsymbol{\Sigma}_{1:2,.} \boldsymbol{\Sigma}_{3,.}^\top\right) \psi^{\mathbb{S}}(l) + \frac{\boldsymbol{\Sigma}_{3,.} \boldsymbol{\Sigma}_{3,.}^\top}{2} \psi^{\mathbb{S}}(l)^2 \Big) \tag{54}$$

As $c(0,t) = I^{1-\alpha}\psi(t)$ and $D^\alpha \psi(t) = \frac{dI^{1-\alpha}\psi(t)}{dt}$, we approach $c(0, t_k)$ by

$$c(k) = \sum_{l=0}^{k-1} \left( \psi_0(\boldsymbol{\omega}) - \left(\kappa - \boldsymbol{\omega}^\top \boldsymbol{\Sigma}_{1:2,.} \boldsymbol{\Sigma}_{3,.}^\top\right) \psi(l) + \frac{\boldsymbol{\Sigma}_{3,.} \boldsymbol{\Sigma}_{3,.}^\top}{2} \psi(l)^2 \right) \Delta \,. \tag{55}$$

and $c^{\mathbb{S}}(0, t_k)$ by

$$c^{\mathbb{S}}(k) = \sum_{l=0}^{k-1} \Big(\psi_0(\boldsymbol{\omega}) + \boldsymbol{\omega}^\top \boldsymbol{\Sigma}_{1:2,.} \boldsymbol{\Sigma}_{1:2,.}^\top \boldsymbol{e}_1 - \left(\kappa^{\mathbb{S}} - \boldsymbol{\omega}^\top \boldsymbol{\Sigma}_{1:2,.} \boldsymbol{\Sigma}_{3,.}^\top\right) \psi^{\mathbb{S}}(l) + \frac{\boldsymbol{\Sigma}_{3,.} \boldsymbol{\Sigma}_{3,.}^\top}{2} \psi^{\mathbb{S}}(l)^2 \Big) \Delta \,. \tag{56}$$

On the other hand, the function $a(0, t_k)$ is calculated from Equation (47) as the following sum

$$a(k) = \sum_{l=0}^{k-1} \left( \boldsymbol{\omega}^\top \left(\boldsymbol{r} - \boldsymbol{\lambda} \odot (\boldsymbol{\varphi}(1) - 1)\right) + \boldsymbol{\lambda}^\top \left(\boldsymbol{\varphi}(\boldsymbol{\omega}) - 1\right) + \kappa\,\theta\,\psi(l) \right) \Delta \,. \tag{57}$$

and

$$a^{\mathbb{S}}(k) = \sum_{l=0}^{k-1} \left( \boldsymbol{\omega}^\top \left(\boldsymbol{r} - \boldsymbol{\lambda} \odot (\boldsymbol{\varphi}(1) - 1)\right) + \boldsymbol{\lambda}^{\mathbb{S}\top} \left(\boldsymbol{\varphi}^{\mathbb{S}}(\boldsymbol{\omega}) - 1\right) + \kappa\,\theta\,\psi^{\mathbb{S}}(l) \right) \Delta \,. \tag{58}$$

We see in the next section how to retrieve the pdf's of claim processes by inverting the mgf with a discrete fast Fourier transform (DFT).

# 7 Probability density functions by DFT

Having found the bivariate characteristic functions of log-returns under $\mathbb{Q}$ and $\mathbb{S}$, we can now turn back to spread and exchange options pricing. We adopt a standard approach that consists to invert characteristic functions by a discrete fast Fourier's transform (DFT) in order to retrieve pdf's.

Let us denote the characteristic function of log-return processes under $\mathbb{Q}$ by $\Upsilon_T(i\boldsymbol{\omega}) = \mathbb{E}\left(e^{i\,\boldsymbol{\omega}^\top \boldsymbol{X}_T} \mid \mathcal{F}_0\right)$ ($\omega \in \mathbb{R}^2$), that is also the inverse Fourier transform of the bivariate probability density function (pdf) $f_{\boldsymbol{X}_T}(\boldsymbol{x})$ of $\boldsymbol{X}_T|\mathcal{F}_0$. Therefore, this density can be retrieved by computing the double integral (the Fourier transform, $\mathcal{F}[.]$, of $\Upsilon_s(.)$):

$$\begin{aligned} f_{\boldsymbol{X}_T}(\boldsymbol{x}) &= \frac{1}{(2\pi)^2}\mathcal{F}[\Upsilon_T(i\boldsymbol{\omega})](\boldsymbol{x}) \\ &= \frac{1}{(2\pi)^2}\int_{-\infty}^{+\infty}\int_{-\infty}^{+\infty}\Upsilon_T(i\boldsymbol{\omega})e^{-i\boldsymbol{\omega}^\top\boldsymbol{x}}d\omega_1 d\omega_2\,. \end{aligned} \tag{59}$$

The calculation of this multiple integral is computationally intensive but it may be speed up if we discretize it in a compatible expression with the DFT, as presented in the next proposition.

**Proposition 7.1.** *Let $M$ be the number of steps used in the discrete fast Fourier Transform (DFT) and $\Delta_x = \frac{2x_{max}}{M}$, be the step of discretization. Let us denote $\Delta_\omega = \frac{2\pi}{M\,\Delta_x}$ and*

$$\boldsymbol{\omega}_{j_1,j_2} = \left(-\frac{M}{2}\Delta_\omega + (j_1-1)\Delta_\omega, -\frac{M}{2}\Delta_\omega + (j_2-1)\Delta_\omega\right)$$

*for $j_1, j_2 \in \{1, ..., M+1\}$. The values of $f_{\boldsymbol{X}_T}(.)$ at points*

$$\boldsymbol{x}_{k_1,k_2} = \left(-\frac{M}{2}\Delta_x + (k_1-1)\Delta_x\,, -\frac{M}{2}\Delta_x + (k_2-1)\Delta_x\right)$$

*for $k_1, k_2 \in \{1, ..., M+1\}$ are approached by*

$$\begin{aligned} f_{\boldsymbol{X}_T}(\boldsymbol{x}_{k_1,k_2}) = Re\Bigg(&\frac{(\Delta_\omega)^2}{(2\pi)^2}e^{-i\pi M + i\pi\sum_{l=1}^2(k_l-1)} \\ &\times\sum_{j_1=1}^{M+1}\sum_{j_2=1}^{M+1}\delta_{j_1,j_2}e^{i\pi\sum_{l=1}^2(j_l-1)}\Upsilon_T\left(i(\boldsymbol{\omega}_{j_1,j_2})\right)e^{-i\sum_{l=1}^2(j_l-1)(k_l-1)\frac{2\pi}{M}}\Bigg)\,, \end{aligned} \tag{60}$$

*where$\Upsilon_T(i\boldsymbol{\omega}) = \mathbb{E}\left(e^{i\,\boldsymbol{\omega}^\top\boldsymbol{X}_T} \mid \mathcal{F}_0\right)$ is defined by equation (46) and*

$$\delta_{j_1,j_2} = \left(\frac{1}{2}\right)^{(1_{\{j_1=1\}}+1_{\{j_2=1\}})}(1 - 1_{\{j_1\neq1,j_2\neq1\}}) + 1_{\{j_1\neq1,j_2\neq1\}}\,.$$

The proof is standard and may be found in e.g. Hainaut ([15]). The expression (60) emphasizes that $f_{\boldsymbol{X}_T}(\boldsymbol{x}_{k_1,k_2})$ is computable with a standard DFT algorithm applied to

$$(\Delta_\omega)^2 \, e^{-i\pi M + i\pi\sum_{l=1}^{2}(k_l-1)} \delta_{j_1,j_2} e^{i\pi\sum_{l=1}^{2}(j_l-1)} \Upsilon_T\left(i(\boldsymbol{\omega}_{j_1,j_2})\right)$$

valued on a 2 dimensional mesh grid. The value of the call-spread option (8) is then approached by the discrete sum

$$\begin{aligned} P^{spread} &= e^{-rT}\sum_{k_1=1}^{M+1}\sum_{k_2=1}^{M+1}\left(\pi_1 S_0^{(1)}e^{x_{k_1}} - \pi_2 S_0^{(2)}e^{x_{k_2}} - K\right) \\ &\quad \times f_{\boldsymbol{X}_T}(\boldsymbol{x}_{k_1,k_2})\,\mathbf{1}_{\{\boldsymbol{x}_{k_1,k_2}\in D^{spread}\}}\,(\Delta_x)^2 \end{aligned}$$

If we refer to Section 2, pricing exchange options requires the computation of the pdf of log-returns difference under $\mathbb{S}$. Let us now denote the characteristic function of log-returns differences under $\mathbb{S}$ by $\Upsilon_{X_T^{(2)}-X_T^{(1)}}(i\omega) = \mathbb{E}^{\mathbb{S}}\left(e^{i\omega\left(X_T^{(2)}-X_T^{(1)}\right)}\,|\,\mathcal{F}_0\right)$ $(\omega\in\mathbb{R})$, that is also the inverse Fourier transform of the bivariate probability density function (pdf) $f^{\mathbb{S}}_{X_T^{(2)}-X_T^{(1)}}(x)$. Therefore, this density can be retrieved by computing the simple integral (the Fourier transform, $\mathcal{F}[.]$, of $\Upsilon_{X_T^{(2)}-X_T^{(1)}}(.)$):

$$\begin{aligned} f^{\mathbb{S}}_{X_T^{(2)}-X_T^{(1)}}(x) &= \frac{1}{2\pi}\mathcal{F}[\Upsilon_{X_T^{(2)}-X_T^{(1)}}(i\omega)](x) \\ &= \frac{1}{2\pi}\int_{-\infty}^{+\infty}\Upsilon_{X_T^{(2)}-X_T^{(1)}}(i\omega)e^{-i\omega x}d\omega. \end{aligned} \tag{61}$$

The calculation of this integral is done by DFT, as presented in the next proposition.

**Proposition 7.2.** *Let $M$ be the number of steps used in the Discrete Fourier Transform (DFT) and $\Delta_x = \frac{2x_{max}}{M}$ be this step of discretization. Let us denote $\Delta_\omega = \frac{2\pi}{M\,\Delta_x}$ and*

$$\omega_j = (j-1)\Delta_\omega,$$

*for $j = 1...M+1$. Let $\Upsilon_{X_T^{(2)}-X_T^{(1)}}(i\omega)$ be mgf of $X_T^{(2)}-X_T^{(1)}$, under $\mathbb{Q}$ or $\mathbb{S}$. The values of $f^{\mathbb{S}}_{X_T^{(2)}-X_T^{(1)}}(.)$ at points $x_k = -\frac{M}{2}\Delta_x + (k-1)\Delta_x$ for $k = 1,...,M+1$ are approached by the sum:*

$$f^{\mathbb{S}}_{X_T^{(2)}-X_T^{(1)}}(x_k) = \frac{2}{M\,\Delta_x}Re\left(\sum_{j=1}^{M}\delta_j\Upsilon_{X_T^{(2)}-X_T^{(1)}}(i\,\omega_j)\,(-1)^{j-1}e^{-i\frac{2\pi}{M}(j-1)(k-1)}\right). \tag{62}$$

*where $\delta_j = \frac{1}{2}1_{\{j=1\}} + 1_{\{j\neq 1\}}$.*

The value of the exchange option (9) is then approached by the sum

$$P^{exchange} = \sum_{k=1}^{M+1}\left(\pi_1 S_0^{(1)} - \pi_2 S_0^{(2)}e^{x_k}\right) f^{\mathbb{S}}_{X_T^{(2)}-X_T^{(1)}}(x_k)\,\mathbf{1}_{\{\boldsymbol{x}_k\in D^{exchange}\}}\,\Delta_x\,,$$

# 8 Numerical illustration

This section studies the influence of the parameter $\alpha$ on the price of spread options for various maturities. Parameters used in this exercise are reported in Table 1. Our main purpose being the study of the impact of roughness on prices, jump processes of both assets are assumed identical and we do not consider Brownian correlation. Notice that removing these assumptions has no impact on conclusions but make less easier the analysis.

| | | | |
|---|---|---|---|
| $r$ | 0.02 | $\theta$ | $0.15^2$ |
| $\kappa$ | 0.80 | $\boldsymbol{\lambda}$ | $\begin{pmatrix} 0.05 & 0.05 \end{pmatrix}^\top$ |
| $\Sigma_{12}$ | $\begin{pmatrix} 1 & 0 & 0 \\ 0 & 1 & 0 \end{pmatrix}$ | $\Sigma_3$ | $\begin{pmatrix} 0 & 0 & 0.2 \end{pmatrix}^\top$ |
| $\eta_{11}$,$\eta_{21}$ | 200 | $\eta_{21}$,$\eta_{22}$ | 100 |
| $p_{11}$,$p_{21}$ | 0.30 | $p_{21}$,$p_{22}$ | 0.70 |
| $S_0^1$ , $S_0^2$ | 100 | $V_0$ | $0.15^2$ |

Table 1: Parameters of the bivariate rough jump diffusion.

Table 2 presents the prices of spread options for various strikes, with $\alpha = 0.9$, 0.7, 0.55 and maturities of 1, 3 and 6 months. This table is obtained by a 2 dimensional (2D) DFT with parameters $x_{max} = 1.4$, $M = 2^7$ and $\Delta_t = 1/350$.

| $T$ | 1/12 | 1/12 | 1/12 | 3/12 | 3/12 | 3/12 | 6/12 | 6/12 | 6/12 |
|---|---|---|---|---|---|---|---|---|---|
| $K \setminus \alpha$ | 0.9 | 0.7 | 0.55 | 0.9 | 0.7 | 0.55 | 0.9 | 0.7 | 0.55 |
| -10 | 10.16 | 10.19 | 10.23 | 11.02 | 11.01 | 11.01 | 12.23 | 12.2 | 12.17 |
| -8 | 8.28 | 8.31 | 8.35 | 9.38 | 9.36 | 9.34 | 10.75 | 10.7 | 10.67 |
| -6 | 6.59 | 6.60 | 6.62 | 7.92 | 7.88 | 7.84 | 9.41 | 9.35 | 9.31 |
| -4 | 4.93 | 4.93 | 4.91 | 6.50 | 6.44 | 6.38 | 8.10 | 8.04 | 7.99 |
| -2 | 3.65 | 3.63 | 3.60 | 5.33 | 5.26 | 5.20 | 6.98 | 6.92 | 6.86 |
| 0 | 2.40 | 2.37 | 2.30 | 4.19 | 4.11 | 4.03 | 5.88 | 5.81 | 5.75 |
| 2 | 1.66 | 1.64 | 1.60 | 3.34 | 3.27 | 3.21 | 5.00 | 4.94 | 4.88 |
| 4 | 0.94 | 0.93 | 0.92 | 2.52 | 2.46 | 2.40 | 4.14 | 4.08 | 4.03 |
| 6 | 0.60 | 0.61 | 0.63 | 1.95 | 1.91 | 1.87 | 3.47 | 3.41 | 3.37 |
| 8 | 0.29 | 0.32 | 0.36 | 1.42 | 1.40 | 1.38 | 2.83 | 2.78 | 2.75 |
| 10 | 0.17 | 0.20 | 0.25 | 1.07 | 1.06 | 1.06 | 2.33 | 2.3 | 2.27 |

Table 2: Prices of spread options by 2D discrete Fourier transform for strikes from -10 up to 10 with rough parameters 0.9, 0.7, 0.55 and maturities 1, 3 and 6 months.

Whatever the maturity, we observe that roughness of the volatility modifies option prices by a few cents. The relative impact, reported in Table 3, depends on strikes and maturities. For 1 month options, the gap between the less and the most rough models climbs at maximum up to 0.08 monetary units. For 6 months options, this gap reaches a maximum of 0.12 monetary units for a strike $K = -2$, that is in relative terms 6.00% of the option value.

| $T$ | 1/12 | 1/12 | 3/12 | 3/12 | 6/12 | 6/12 |
|---|---|---|---|---|---|---|
| $K \setminus \alpha$ | 0.7 | 0.55 | 0.7 | 0.55 | 0.7 | 0.55 |
| -10 | 0.30 | 0.72 | -0.03 | -0.09 | -0.26 | -0.46 |
| -8 | 0.35 | 0.83 | -0.23 | -0.47 | -0.41 | -0.73 |
| -6 | 0.19 | 0.43 | -0.51 | -1.02 | -0.57 | -1.02 |
| -4 | -0.12 | -0.35 | -0.92 | -1.82 | -0.79 | -1.41 |
| -2 | -0.59 | -1.60 | -1.30 | -2.58 | -0.97 | -1.73 |
| 0 | -1.56 | -4.15 | -1.87 | -3.72 | -1.22 | -2.18 |
| 2 | -1.30 | -3.52 | -2.07 | -4.11 | -1.36 | -2.42 |
| 4 | -0.61 | -1.84 | -2.38 | -4.7 | -1.54 | -2.75 |
| 6 | 2.14 | 4.69 | -2.07 | -4.12 | -1.55 | -2.77 |
| 8 | 10.04 | 23.52 | -1.52 | -3.10 | -1.56 | -2.78 |
| 10 | 17.34 | 41.87 | -0.36 | -0.93 | -1.35 | -2.43 |

Table 3: Relative gaps in % between prices of spread options with rough parameters 0.7, 0.55 with respect to prices with $\alpha = 0.90$, i.e. $\frac{Price(\alpha=0.55 \, or \, \alpha=0.70) - Price(\alpha=0.90)}{Price(\alpha=0.90)}$.

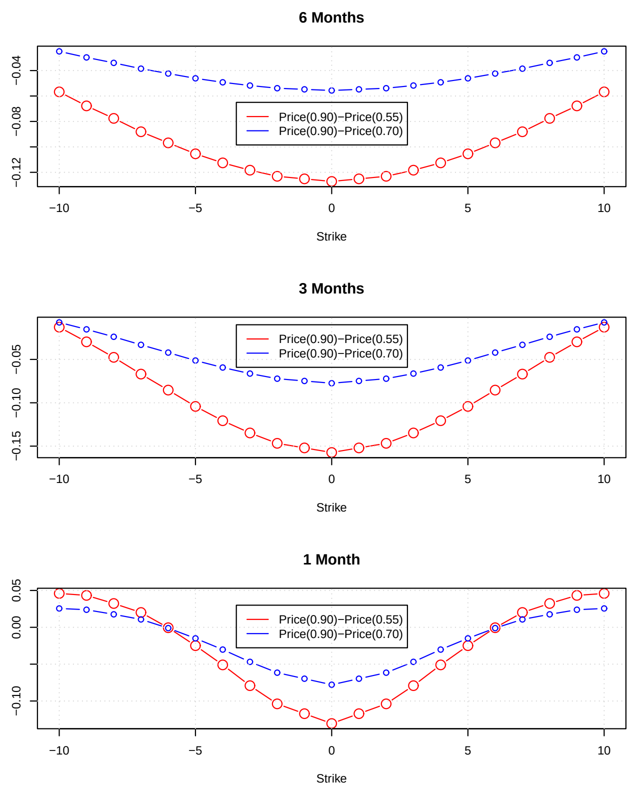


Figure 1: Gaps (in monetary units) between option prices of same maturities for various degrees of roughness.

We also notice that more roughness in the volatility does not systematically increase option prices. This point is emphasized by Figures 1 and 2 that plot the absolute and relative gaps between option prices of same maturities with different degrees of roughness. For "at the money" options ($K = 0$), prices with a roughness parameter $\alpha$=0.55, are lower than these computed in a less rough model with $\alpha = 0.90$. The relative gap respectively ranges from -4.15% up to -2.18% for maturities of 1 and 3 months. For 1 month deep in or out of the money options, increasing the level of roughness slightly raises prices as revealed by the third subplot of Figure 1. Notice that the highest relative gaps are achieved for out of the money options computed with $\alpha = 0.55$ and $\alpha = 0.90$ that are also the cheapest ones.

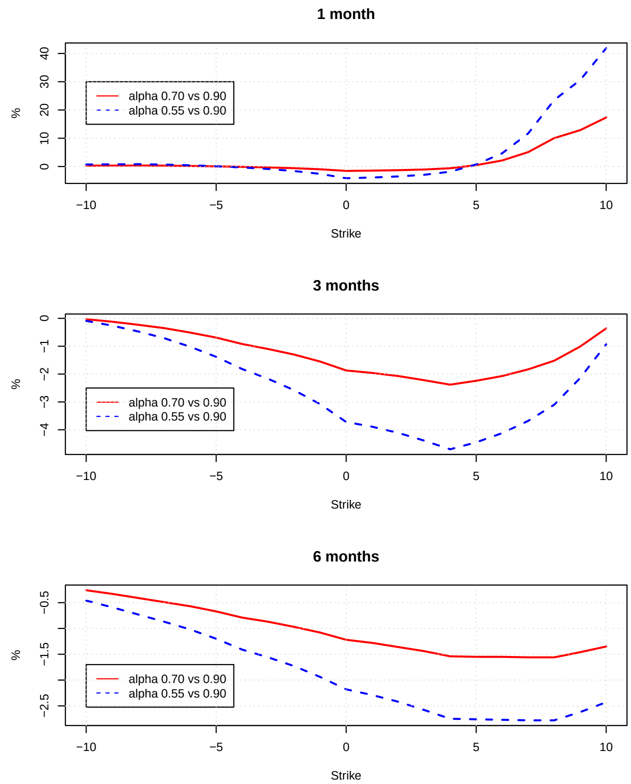


Figure 2: Relative gaps (in %) between option prices of same maturities for various degrees of roughness.

Table 6 in Appendix C reports spread option prices computed with 10,000 Monte Carlo simulations. Table 6 of the same appendix shows the relative errors (in %) between DFT and Monte-Carlo prices of spread options. We observe that the DFT pricing error is smaller than 1% for most of "at" or "in" the money options. For out of the money options, the error may reach 10% or more but this corresponds to a few cents in absolute value. Nevertheless, this emphasizes the lack of accuracy of the DFT method for pricing "out" of the money spread options. Using a thinner grid (small $\Delta_x$) should improve accuracy. Nevertheless, it increases the ranges of $\omega_j$ in Proposition 7.2 since $\Delta_\omega \Delta_x = \frac{2\pi}{M}$. For large $\omega_j$, solving the fractional differential equation (50) is numerically unstable.

The analysis of Table 6 confirms our conclusions based on DFT prices that more roughness does not systematically raise option prices. Table 8 of Appendix C compares spread option prices in the non-rough jump Heston model to prices in its rough counterpart with $\alpha = 0.9$. The comparison is based on prices obtained with 10,000 simulations. We again observe that increasing roughness leads to a reduction of spread option prices. This decrease of price is caused by the short memory of the rough volatility. It "forgets" previous peaks of volatility at a faster pace than its non-rough counterpart. The volatility in the rough model has well a more chaotic sample path than in the non-rough Heston but it globally reverts quicker to its baseline level. The volatility being lower on average, this drives down option prices. This is confirmed by Table 4 that compares averages of daily simulated standard deviations, $\sqrt{V_t}$ in rough and non-rough models over 1 year (10,000 simulations). For the jump-Heston model with parameters of Table 2, we obtain an average standard deviations of 14.07% whereas the rough model with $\alpha = 0.55$ gives us a an average of 12.20%. As expected, the volatility of $\sqrt{V_t}$ when $\alpha = 0.55$ is nevertheless higher than the one of the non rough model.

| | $\alpha = 1$ | $\alpha = 0.90$ | $\alpha = 0.70$ | $\alpha = 0.55$ |
|---|---|---|---|---|
| average | 0.1407 | 0.1392 | 0.1323 | 0.1220 |
| standard deviation | 0.0557 | 0.0594 | 0.0732 | 0.0903 |
| 5% percentile | 0.0478 | 0.0446 | 0.0230 | 0.0000 |
| 95% percentile | 0.2347 | 0.2416 | 0.2627 | 0.2885 |

Table 4: Average, standard deviations and percentiles of simulated $\sqrt{V_t}$ (daily steps) over 1 year.

Table 5 reports exchange options for various degrees of roughness and maturities computed with the 1 dimensional (1D) DFT of Proposition 7.2. They are compared to prices obtained with 10,000 Monte-Carlo simulations (here under the $\mathbb{S}$ measure) and with the 2D DFT ( $x_{max} = 1.4$, $M = 2^7$ and $\Delta_t = 1/350$). While the 2D DFT achieves an excellent accuracy, we observe that the 1D DFT significantly underestimates prices, in particular for short term maturities. This is explained by the insufficient granularity of the mesh on which we approach the density $f_{X_T^{(2)} - X_T^{(1)}}(.)$. In practise, using a thinner grid (small $\Delta_x$) increases the ranges of $\omega_j$ in Proposition 7.2 since $\Delta_\omega \Delta_x = \frac{2\pi}{M}$. For large $\omega_j$, solving the fractional differential equation (50) becomes numerically unstable and even with a very small $\Delta$, the approximation (53) diverges.

| $\alpha$ | $M$ | $x_{max}$ | Expiry 1/12 | 3/12 | 6/12 |
|---|---|---|---|---|---|
| 0.9 | $2^6$ | 0.6 | 2.0000 | 3.7089 | 5.3482 |
| 0.9 | $2^7$ | 0.6 | 2.1981 | 3.8354 | 5.5531 |
| 0.9 | $2^8$ | 1.1 | 2.2160 | 3.8547 | 5.5853 |
| 0.9 | M.C. | | 2.4109 | 4.1512 | 5.8168 |
| 0.9 | 2D | | 2.4029 | 4.1864 | 5.8825 |
| 0.7 | $2^6$ | 0.6 | 1.9500 | 3.6293 | 5.2637 |
| 0.7 | $2^7$ | 0.6 | 2.1453 | 3.8354 | 5.4695 |
| 0.7 | $2^8$ | 1.1 | 2.1633 | 3.7777 | 5.5147 |
| 0.7 | M.C. | | 2.3743 | 4.0964 | 5.7849 |
| 0.7 | 2D | | 2.3653 | 4.1083 | 5.8107 |
| 0.55 | $2^6$ | 0.6 | 1.8776 | 3.5516 | 5.1971 |
| 0.55 | $2^7$ | 0.6 | 2.0691 | 3.7569 | 5.1971 |
| 0.55 | $2^8$ | 1.1 | 2.0867 | 3.7777 | 5.4569 |
| 0.55 | M.C. | | 2.3401 | 4.0658 | 5.8014 |
| 0.55 | 2D | | 2.3031 | 4.0307 | 5.7545 |

Table 5: Prices of exchange options obtained with the 1D DFT, maturities 1, 3 and 6 months.

# 9 Conclusions

To the best of our knowledge, this article is among the first to study the pricing of spread and exchange options in a bivariate rough jump Heston model. We find the joint characteristic function of log-returns in terms of solutions of fractional differential equations. Results are provided under the risk neutral measure and under a measure using a risky asset as numeraire. Compared to the existing literature, our approach is simple and based on the limit of a discretized model and on a discrete approximation of Riemann-Liouville derivatives.

The numerical illustration allows us to draw several interesting conclusions. Firstly, the 2D DFT achieves a good accuracy for prices of "in" and "at" the money options. For options far "out" of the money, the pricing error by DFT is non-negligible and in this case, we should favour Monte-Carlo pricing. Secondly, a higher level of roughness in stock prices volatility does not systematically increases option prices. This is explainable by the short memory of rough volatility sample paths. The volatility in the rough model has well a more chaotic sample path than in the non-rough Heston but it globally reverts quicker to its baseline level. The volatility being lower on average, this drives down option prices. Finally, we show that using a 1D DFT for valuing exchange options, that is in theory numerically more efficient, leads to higher pricing errors than the 2D DFT. In theory, increasing the granularity reduces errors but using a thinner grid causes numerical instabilities in the solving of fractional differential equations.

This article paves the way for further research. Firstly, the methodology used for finding the characteristic function of log-returns may be applied to many other market models than the rough Heston framework. Secondly, the finite difference method solving fractional differential equations may probably be improved. Based on Momani and Shawagfeh [21], we can for instance try the Adomian decomposition method combined with Padé approximants to numerically solves these equations.

# Appendix A

We prove in this appendix that $L_t^{X(1)}$ is a compound Poisson process with parameters $\lambda_1^{\mathbb{S}} = \lambda_1 \varphi^{(1)}(1)$, $p_{11}^{\mathbb{S}}$, $p_{12}^{\mathbb{S}}$, $\eta_{11}^{\mathbb{S}}$, $\eta_{12}^{\mathbb{S}}$ such as defined in Equations (19) and (20). For this purpose, we develop the moment generating function (mgf) of $L_t^{X(1)} = \sum_{k=1}^{N_t^{(1)}} J_k^{(1)}$ under the $\mathbb{S}$ measure:

$$\begin{aligned}\mathbb{E}^{\mathbb{S}}\left(e^{\omega L_t^{X(1)}}|\mathcal{F}_0\right) &= \mathbb{E}\left(\left.\frac{d\mathbb{S}}{d\mathbb{Q}}\right|_t e^{\omega L_t^{X(1)}}|\mathcal{F}_0\right) \\ &= e^{-\lambda_1\left(\varphi^{(1)}(1)-1\right)t}\mathbb{E}\left(e^{\sum_{k=1}^{N_t^{(1)}}(1+\omega)J_k^{(1)}}|\mathcal{F}_0\right) \\ &= \exp\left(\left(\lambda_1\varphi^{(1)}(1)\right)t\left(\frac{\mathbb{E}\left(e^{(1+\omega)J^{(1)}}\right)}{\varphi^{(1)}(1)}-1\right)\right)\,.\end{aligned} \tag{63}$$

The expectation $\mathbb{E}\left(e^{(1+\omega)J^{(1)}}\right)/\varphi^{(1)}(1)$ can be rewritten as follows

$$\begin{aligned}\frac{\mathbb{E}\left(e^{(1+\omega)J^{(1)}}\right)}{\varphi^{(1)}(1)} &= \frac{p_{11}}{\varphi^{(1)}(1)}\frac{\eta_{11}}{\eta_{11}-\omega-1} + \frac{p_{12}}{\varphi^{(1)}(1)}\frac{\eta_{12}}{\eta_{12}+\omega+1} \\ &= \frac{\eta_{11}p_{11}}{\varphi^{(1)}(1)\left(\eta_{11}-1\right)}\left(\frac{(\eta_{11}-1)}{(\eta_{11}-1)-\omega}\right) + \frac{\eta_{12}p_{12}}{\varphi^{(1)}(1)\left(\eta_{12}+1\right)}\left(\frac{(\eta_{12}+1)}{(\eta_{12}+1)+\omega}\right)\,.\end{aligned}$$

Since $p_{11}\frac{\eta_{11}}{\eta_{11}-1} + p_{12}\frac{\eta_{12}}{\eta_{12}+1} = \varphi^{(1)}(1)$, $p_{11}^{\mathbb{S}} = \frac{\eta_{11}p_{11}}{\varphi^{(1)}(1)(\eta_{11}-1)}$ and $p_{12}^{\mathbb{S}} = \frac{\eta_{12}p_{12}}{\varphi^{(1)}(1)(\eta_{12}+1)}$ are well in $[0,1]$ and such that $p_{11}^{\mathbb{S}} + p_{12}^{\mathbb{S}} = 1$. We infer that $\mathbb{E}\left(e^{(1+\omega)J^{(1)}}\right)/\varphi^{(1)}(1)$ is the moment generating a double exponential random variable with parameters $p_{11}^{\mathbb{S}}$, $p_{12}^{\mathbb{S}}$, $\eta_{11}^{\mathbb{S}}$, $\eta_{12}^{\mathbb{S}}$. From Equation (63), we recognize the mgf of a compound Poisson process with a jump intensity equal to $\lambda_1^{\mathbb{S}}$.

# Appendix B

This appendix presents the characteristic of log-returns under $\mathbb{Q}$ and $\mathbb{S}$ when the variance process is ruled by a Cox-Ingersoll-Ross (CIR) process, as defined by Equation (7).

**Proposition 9.1.** *For $\boldsymbol{\omega} = (\omega_1, \omega_2)^\top \in \mathbb{C}^{2,-}$ and $0 \le t \le s$, the characteristic function of log-returns $\boldsymbol{X}_s = (X_s^{(1)}, X_s^{(2)})$ under the risk neutral measure if $V_t$ is driven by Equation (7),* *is*

$$\mathbb{E}\left(e^{\boldsymbol{\omega}^\top \boldsymbol{X}_s}|\mathcal{F}_t\right) = \exp\left(a(t,s) + c(t,s)V_t + \boldsymbol{\omega}^\top \boldsymbol{X}_t\right) \tag{64}$$

*where functions $a(t,s)$, $c(t,s)$ solve the following ordinary differential equations (ODE's):*

$$\partial_t a(t,s) = -\boldsymbol{\omega}^\top\left(\boldsymbol{r} - \boldsymbol{\lambda}\odot(\boldsymbol{\varphi}(1)-1)\right) - \boldsymbol{\lambda}^\top\left(\boldsymbol{\varphi}(\boldsymbol{\omega})-1\right) - \kappa\,\theta\,c(t,s)\,, \tag{65}$$

*and*

$$\begin{aligned}\partial_t c(t,s) &= \frac{1}{2}\boldsymbol{\omega}^\top diag(\boldsymbol{\Sigma}_{1:2,.}\boldsymbol{\Sigma}_{1:2,.}^\top) - \frac{1}{2}\boldsymbol{\omega}^\top\left(\boldsymbol{\Sigma}_{1:2,.}\boldsymbol{\Sigma}_{1:2,.}^\top\right)\boldsymbol{\omega} \\ &+ \left(\kappa - \boldsymbol{\omega}^\top\boldsymbol{\Sigma}_{1:2,.}\boldsymbol{\Sigma}_{3,.}^\top\right)c(t,s) - \frac{\boldsymbol{\Sigma}_{3,.}\boldsymbol{\Sigma}_{3,.}^\top}{2}c(t,s)^2\end{aligned} \tag{66}$$

*with the terminal conditions $a(s,s) = 0$ and $c(s,s) = 0$.*

**Proposition 9.2.** *For $\boldsymbol{\omega} = (\omega_1,\omega_2)^\top \in \mathbb{C}^{2,-}$ and $0 \le t \le s$ and if if $V_t$ is driven by Equation (7), the characteristic function of log-returns $\boldsymbol{X}_s = (X_s^{(1)}, X_s^{(2)})$ under the $\mathbb{S}$ measure is*

$$\mathbb{E}^{\mathbb{S}}\left(e^{\boldsymbol{\omega}^\top \boldsymbol{X}_s}|\mathcal{F}_t\right) = \exp\left(a^{\mathbb{S}}(t,s) + c^{\mathbb{S}}(t,s)V_t + \boldsymbol{\omega}^\top \boldsymbol{X}_t\right) \tag{67}$$

*If we note $\lambda_1^{\mathbb{S}} = \lambda_1\varphi^{(1)}(1)$ , $\kappa^{\mathbb{S}} = \kappa - \boldsymbol{\Sigma}_{3,.}\boldsymbol{\Sigma}_{1:2,.}^\top\boldsymbol{e}_1$, the functions $a^{\mathbb{S}}(t,s)$, $c^{\mathbb{S}}(t,s)$ solve the following ordinary differential equations (ODE's):*

$$\partial_t a^{\mathbb{S}}(t,s) = -\boldsymbol{\omega}^\top\left(\boldsymbol{r} - \boldsymbol{\lambda}\odot(\boldsymbol{\varphi}(1)-1)\right) - \boldsymbol{\lambda}^{\mathbb{S}\top}\left(\boldsymbol{\varphi}^{\mathbb{S}}(\boldsymbol{\omega})-1\right) - \kappa\,\theta\,c^{\mathbb{S}}(t,s)\,, \tag{68}$$

*and*

$$\begin{aligned}\partial_t c^{\mathbb{S}}(t,s) &= -\boldsymbol{\omega}^\top\left(\boldsymbol{\Sigma}_{1:2,.}\boldsymbol{\Sigma}_{1:2,.}^\top\boldsymbol{e}_1 - \frac{1}{2}diag(\boldsymbol{\Sigma}_{1:2,.}\boldsymbol{\Sigma}_{1:2,.}^\top)\right) - \frac{1}{2}\boldsymbol{\omega}^\top\left(\boldsymbol{\Sigma}_{1:2,.}\boldsymbol{\Sigma}_{1:2,.}^\top\right)\boldsymbol{\omega} \\ &+ \left(\kappa^{\mathbb{S}} - \boldsymbol{\omega}^\top\boldsymbol{\Sigma}_{1:2,.}\boldsymbol{\Sigma}_{3,.}^\top\right)c^{\mathbb{S}}(t,s) - \frac{\boldsymbol{\Sigma}_{3,.}\boldsymbol{\Sigma}_{3,.}^\top}{2}c(t,s)^2\end{aligned} \tag{69}$$

*with the terminal conditions $a(s,s) = 0$ and $c(s,s) = 0$.*

# Appendix C

| $T$ | 1/12 | 1/12 | 1/12 | 3/12 | 3/12 | 3/12 | 6/12 | 6/12 | 6/12 |
|---|---|---|---|---|---|---|---|---|---|
| $K \setminus \alpha$ | 0.9 | 0.7 | 0.55 | 0.9 | 0.7 | 0.55 | 0.9 | 0.7 | 0.55 |
| -10 | 10.14 | 10.16 | 10.18 | 10.98 | 10.99 | 10.97 | 12.2 | 12.22 | 12.25 |
| -8 | 8.27 | 8.29 | 8.31 | 9.35 | 9.35 | 9.33 | 10.71 | 10.72 | 10.75 |
| -6 | 6.52 | 6.52 | 6.54 | 7.85 | 7.82 | 7.81 | 9.32 | 9.32 | 9.35 |
| -4 | 4.93 | 4.91 | 4.91 | 6.47 | 6.43 | 6.41 | 8.04 | 8.03 | 8.06 |
| -2 | 3.55 | 3.52 | 3.49 | 5.23 | 5.19 | 5.15 | 6.86 | 6.85 | 6.87 |
| 0 | 2.41 | 2.38 | 2.34 | 4.15 | 4.10 | 4.07 | 5.81 | 5.78 | 5.81 |
| 2 | 1.55 | 1.52 | 1.49 | 3.23 | 3.18 | 3.15 | 4.87 | 4.84 | 4.86 |
| 4 | 0.94 | 0.92 | 0.91 | 2.47 | 2.43 | 2.41 | 4.04 | 4.02 | 4.04 |
| 6 | 0.53 | 0.53 | 0.55 | 1.85 | 1.83 | 1.82 | 3.33 | 3.31 | 3.33 |
| 8 | 0.28 | 0.29 | 0.32 | 1.36 | 1.36 | 1.36 | 2.73 | 2.71 | 2.73 |
| 10 | 0.14 | 0.16 | 0.18 | 0.99 | 1.00 | 1.01 | 2.21 | 2.21 | 2.23 |

Table 6: Prices of spread options by Monte-Carlo for strikes from -10 up to 10 with rough parameters 0.9, 0.7, 0.55 and maturities 1, 3 and 6 months.

| $T$ | 1/12 | 1/12 | 1/12 | 3/12 | 3/12 | 3/12 | 6/12 | 6/12 | 6/12 |
|---|---|---|---|---|---|---|---|---|---|
| $K \setminus \alpha$ | 0.9 | 0.7 | 0.55 | 0.9 | 0.7 | 0.55 | 0.9 | 0.7 | 0.55 |
| -10 | 0.20 | 0.30 | 0.49 | 0.36 | 0.18 | 0.36 | 0.25 | 0.16 | 0.65 |
| -8 | 0.12 | 0.24 | 0.48 | 0.32 | 0.11 | 0.11 | 0.37 | 0.19 | 0.74 |
| -6 | 1.07 | 1.23 | 1.22 | 0.89 | 0.77 | 0.38 | 0.97 | 0.32 | 0.43 |
| -4 | 0.00 | 0.41 | 0.00 | 0.46 | 0.16 | 0.47 | 0.75 | 0.12 | 0.87 |
| -2 | 2.82 | 3.12 | 3.15 | 1.91 | 1.35 | 0.97 | 1.75 | 1.02 | 0.15 |
| 0 | 0.41 | 0.42 | 1.71 | 0.96 | 0.24 | 0.98 | 1.20 | 0.52 | 1.03 |
| 2 | 7.10 | 7.89 | 7.38 | 3.41 | 2.83 | 1.90 | 2.67 | 2.07 | 0.41 |
| 4 | 0.00 | 1.09 | 1.10 | 2.02 | 1.23 | 0.41 | 2.48 | 1.49 | 0.25 |
| 6 | 13.21 | 15.09 | 14.55 | 5.41 | 4.37 | 2.75 | 4.2 | 3.02 | 1.20 |
| 8 | 3.57 | 10.34 | 12.5 | 4.41 | 2.94 | 1.47 | 3.66 | 2.58 | 0.73 |
| 10 | 21.43 | 25.00 | 38.89 | 8.08 | 6.00 | 4.95 | 5.43 | 4.07 | 1.79 |

Table 7: Relative errors (in %) between DFT and Monte-Carlo (M.C.) prices of spread options, i.e. $\frac{Price(DFT)-Price(M.C.)}{Price(DFT)}$

| | Prices | | | Relative changes (%) $\alpha = 0.9$ vs $\alpha = 1$ | | |
|---|---|---|---|---|---|---|
| $K \backslash T$ | 1/12 | 1/12 | 1/12 | 3/12 | 3/12 | 3/12 |
| -10 | 10.33 | 11.51 | 13.21 | -0.02 | -0.05 | -0.17 |
| -8 | 8.46 | 9.86 | 11.68 | -0.02 | -0.05 | -0.2 |
| -6 | 6.69 | 8.32 | 10.23 | -0.03 | -0.06 | -0.24 |
| -4 | 5.08 | 6.9 | 8.88 | -0.03 | -0.06 | -0.28 |
| -2 | 3.68 | 5.63 | 7.64 | -0.04 | -0.07 | -0.33 |
| 0 | 2.52 | 4.5 | 6.52 | -0.04 | -0.08 | -0.38 |
| 2 | 1.63 | 3.53 | 5.51 | -0.05 | -0.09 | -0.43 |
| 4 | 1 | 2.72 | 4.62 | -0.06 | -0.09 | -0.48 |
| 6 | 0.57 | 2.06 | 3.84 | -0.06 | -0.1 | -0.53 |
| 8 | 0.3 | 1.52 | 3.17 | -0.06 | -0.11 | -0.57 |
| 10 | 0.15 | 1.11 | 2.59 | -0.05 | -0.11 | -0.61 |

Table 8: Prices of spread options by Monte-Carlo in the Heston model with jumps ($\alpha = 1$) and relative gaps with respect to prices for $\alpha = 0.9$, i.e. $\frac{Price(\alpha=0.9)-Price(\alpha=1)}{Price(\alpha=0.9)}$.

# References


[1] Abi Jaber E., Larsson M., Pulido S. 2019. Affine volterra processes, Annals of Applied Probability 29 (5), 3155–3200

[2] Abi Jaber, E., El Euch O. 2019. Multi-factor approximation of rough volatility models. SIAM Journal of Financial Mathematics , 10(2), 309–349.

[3] Alfeus M., Schlögl E., 2019. On spread option pricing using two-dimensional Fourier transform. Journal of Theoretical and Applied Finance, 22 (5), 1950023.

[4] Bayer C., Friz P., Gatheral J. 2016. Pricing under rough volatility. Quantitative Finance, 16 (6), 887–904.

[5] Bjerksund P., Stensland G. 2014. Closed form spread option valuation. Quantitative Finance, 14 (10), 1785-1794.

[6] Caldana R., Fusai G., 2013. A general closed-form spread option pricing formula, Journal of Banking & Finance, 37, 4893–4906.

[7] Carmona R., Durrleman V. 2003. Pricing and hedging spread options, SIAM Review, 45 , 627–685.

[8] Deelstra G., Petkovic A., Vanmaele M., 2010. Pricing and hedging Asian basket spread options. Journal of computational and applied mathematics, 233 (11), 2814-2830.

[9] Dempster M.A., Hong S.S. 2000. Spread option valuation and the fast Fourier transform. Mathematical Finance—Bachelier Congress 2000, Springer, Berlin, 2002, 203–220.

[10] Dupret J.L., Barbarin J., Hainaut D. 2021. Impact of rough stochastic volatility models on long-term life insurance pricing. Forthcoming in European Actuarial Journal.

[11] Dupret J.L., Hainaut D. 2021. Portfolio insurance under rough volatility and Volterra processes. Forthcoming in International Journal of Theoretical and Applied Finance.

[12] El Euch, O., Rosenbaum, M. 2018. Perfect hedging in rough heston models. The Annals of Applied Probability 28(6), 3813–3856.

[13] El Euch O., Rosenbaum M. 2019. The characteristic function of rough heston models, Mathematical Finance 29 (1), 3–38.

[14] Gatheral J. Jaisson T., Rosenbaum M. 2018. Volatility is rough, Quantitative Finance 18 (6), 933–949.

[15] Hainaut D. 2021. Moment generating function of non-Markov self-excited claims processes. Insurance: Mathematics & Economics, 101 (B), 406-424.

[16] Hurd T.R. , Zhou Z., 2010. A Fourier Transform Method for Spread Option Pricing. SIAM Journal of Financial Mathematics, 1, pp. 142–157.

[17] Kirk E. 1995. Correlations in the energy markets. Managing Energy Price Risk, Risk Publications and Enron, London, 1995, pp. 71–78.

[18] Li M., Deng S., Zhou J. 2008. Closed-form approximations for spread option prices and Greeks. Journal of Derivatives, 15, pp. 58–80.

[19] Margrabe W., 1978. The Value of an Option to Exchange One Asset for Another, Journal of Finance, 33 (1), pp. 177-186.

[20] Merhdoust F., Najafi A.R., Fallah S., Samimi O. 2018. Mixed fractional Heston model and the pricing of American options. Journal of Computational and Applied Mathematics, 330 (1), 141-154.

[21] Momani S., Shawagfeh N. 2006. Decomposition method for solving fractional riccati differential equations. Applied Mathematics and Computation, 182 (2), 1083–1092.

[22] Pasricha P., Goel A., 2019. Pricing vulnerable power exchange options in an intensity based framework. Journal of Computational and Applied Mathematics, 355 (1), 106-115.

[23] Sun Y., Xu C. 2018. A hybrid Monte Carlo acceleration method of pricing basket options based on splitting. Journal of Computational and Applied Mathematics, 342, 292-304.